

AD655637
AD655637

Final Report

EFFECTS OF MULTIPLE PATHS ON ACOUSTICAL SIGNALS

By

Dwight Wayne Batteau

401 3/0

Reproduction in whole or in part is
permitted by the U.S. Government.

Distribution of this document is unlimited.

June 15, 1967

work performed under
Contract Number NONR 494 (20)
U.S. Navy Office of Naval Research

DDIC
RECEIVED
AUG 7 1967
A

Department of Mechanical Engineering
Tufts University
Medford, Massachusetts

RECEIVED

AUG 8 1967

CFSTI

83

CONTENTS -- PREVIOUS REPORTS AND THIS FINAL REPORT

Previous reports under this contract:

Progress Report of 18 Jan. 1967, 1 page letter to Head,
Physiological Psychology Branch, ONR, from D.W. Batteau.

Final Report, 1 June 1966

Section I. D.W. Batteau, "A study of acoustical multipath
systems" 7 pages, 1 June 1966.

Section II. H. Geoffrey Fisher, "Subjective Testing"
16 pages, 1 June 1966.

Section III. Harald Robinson and William van Lennep,
"Apparatus and devices" 21 pages, 1 June 1966.

Section IV. D.W. Batteau and G. Patrick Flanagan,
"Delay Line" 16 pages, 1 June 1966.

Status Report of 1 Sept. 1966, 3-page letter to Commander,
Code 454, Physiological Psychology Branch, ONR, from
Peter R. Markey.

Progress Report, 1 January 1967, 3-page letter to Commander,
Code 454, Physiological Psychology Branch, ONR, from
Peter R. Markey.

Contents of this Final Report:

Introduction.

Résumé of considerations.

Conclusions.

"On the electrical generation and sensing of rotational stress waves
in metal wire delay lines" Philip Yang and Lloyd Trefethen,
20 pages, 6 October 1966.

"Three dimensional stress-strain-magnetic field relations for an
isotropic ferromagnetic material" Philip Yang, 18 pages,
9 November 1967.

"An analytical and experimental study of magnetostrictive delay
lines" Philip Yang, 18 pages, January 1967.

"Magnetic current twist of magnetostriction material contrasted
with Wiedmann's twist" Philip Yang, 20 pages, February 1967.

INTRODUCTION

In the studies of the effects of multiple path systems, difficulties were encountered in conducting tests and in computer programming. The difficulties were (1) problems in the systematic conduct of outlined testing procedures, (2) problems in the construction of apparatus for scheduled tests, and (3) problems with digitizing taped signals for computer programming. These were in part due to diversion of interest on the part of personnel assigned to the tasks and in part to equipment problems in the Adage, Inc. equipment rented for digitizing. However, the results obtained in the study of acoustical delay lines, aimed towards their use in signal processing, may have some merit. This material is presented in the attached reports of the Tufts University Department of Mechanical Engineering.

RÉSUMÉ OF CONSIDERATIONS

Based on the studies of the human pinna, and following the mathematical formulation of that function, it has been shown that the redundant signals in acoustical multipath systems may be processed to improve intelligibility and to do so selectively to location of the source of the signals.

In order to provide studies leading to the utilization of these facts, duplicate pinna and mounts were constructed, a system of multiple microphones was designed, and reverberant studies using room reverberation and reverberation synthesized by delay line were outlined. (As previously mentioned, difficulties prevented the realization of these studies.)

In order to systematize the work, it was scheduled as follows:

1. Comparison tests of microphones with and without pinnae.
2. Comparison tests of single microphones and multiple arrays.

3. Comparison tests of computed attention
and uncomputed reverberation.

I still believe that pursuit of such a program under proper conditions would be extremely useful.

In order to provide data, word list tapes were prepared for use in deriving intelligibility statistics and are available.

In order to provide delay lines of use in the program, studies were initiated which led to the attached reports.

CONCLUSIONS

It is still conceivable that the use of wire delays, digitizing and machine computation on reverberant signals will provide selection and improved intelligibility. However, it is also concluded that such work must be pursued in an environment where the purposes of the research can be systematically followed.

TUFTS UNIVERSITY MECHANICAL ENGINEERING REPORT

NUMBER T.U.M.E.R. 66-2

ON THE ELECTRICAL GENERATION AND SENSING OF ROTATIONAL
STRESS WAVES IN METAL WIRE DELAY LINES

by Philip Yang and Lloyd Trefethen, 6 October 1966

ABSTRACT

A model is proposed for the mechanism of the origin of the rotational stress waves in a wire when an unsteady voltage is supplied to a coil around the wire and a steady state current is supplied to the wire. The relationship of the voltage at the output coil to the voltage at the input coil was derived as:

$$V_2 = \frac{g N_2 (\mu + 1) I_0 \rho^{1/2} \ell_1}{2 \pi^2 R N_1 G_n^{3/2}}$$

Further study is needed to examine the validity of the assumptions made.

CONTENTS

- I. INTRODUCTION
 - II. QUASI-STATIC MAXWELL EQUATIONS FOR AN ELECTRO-MECHANICAL SYSTEM
 - III. BODY-FORCES DUE TO THE MAGNETIC INPUT
 - IV. TORQUE AND ANGULAR DISPLACEMENT
 - V. STRESS WAVE PROPAGATION AND OUTPUT VOLTAGE
 - VI. CONCLUSION
- APPENDIX A: MAXWELL EQUATIONS FOR AN ELECTRO-MAGNETIC SYSTEM
- APPENDIX B: DERIVATION OF ANGULAR DISPLACEMENT $\theta(t)$
- REFERENCE

APPENDIX
NOMENCIATURE

J	current density, Amperes/meter ²
\bar{n}	outward normal vector indicating direction only
$S(a)$	area, meter ²
V	Volume, meter ³
ρ_c	charge density, Coulombs/meter ³
\bar{f}	force density, Newtons/meter ³
\bar{E}	electric field intensity, volt/meter
\bar{B}	induced magnetic field density, Gauss/meter ²
\bar{H}	applied magnetic field density, Gauss/meter ²
\bar{D}	electric displacement vector, Coulombs/meter ²
μ	permeability constant
ϵ	dielectric constant
$\nabla\mu$	gradient of $\mu(x,y,z)$, $\frac{\partial\mu}{\partial x}\bar{i} + \frac{\partial\mu}{\partial y}\bar{j} + \frac{\partial\mu}{\partial z}\bar{k}$
N_1	No. of turns at input coil
N_2	No. of turns at output coil
l_1	length of input coil, meters
l_2	length of output coil, meters
$i_1(t)$	current at input coil, Amperes
$V_1(t)$	voltage at input coil, volts
I_0	steady current through the nickel line, Amperes
R	radius of the nickel line
F_s	force in the rotational direction, Newtons

T_s torque, Newton meter

θ angular rotation (displacement)

$\left(\frac{d\theta}{dx}\right)$ constant strain, degree/meter

G_n shear modulus of nickel, Newtons/meter²

$C = \sqrt{\frac{G_n}{\rho}}$ speed of propagation, meter/sec

D.t. delay time, sec.

I INTRODUCTION

A nickle-wire delay line was developed by D. W. Batteau and G. P. Flanagan, initially suggested by observations by students in a senior projects laboratory course; subsequently, it was found that H. Whitehouse and others at N.O.T.S., Pasadena, had been working on such a delay line for some time. (1). At this time, details of the N.O.T.S. delay line, and of the ideas of that group, have not been available; H. Whitehouse has suggested background references which will be studied, and which will undoubtedly change appreciably the pattern of ideas here adopted as a tentative model of operation of the delay line. Additionally, one of us (Phillip Yang) intends shortly to visit N.O.T.S. for the purpose of discussing these phenomena. In particular, one reference which has been glanced at suggests that a quite different explanation for the initial twist than that detailed in Appendix B may be applicable.

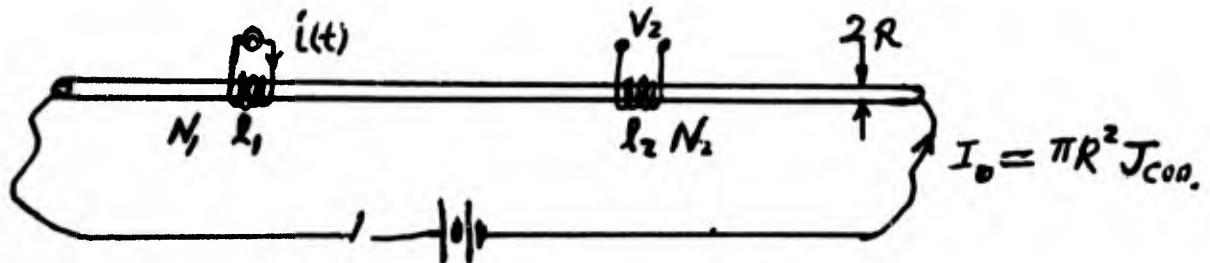
The observation originally made by students was that a nickle wire carrying a d.c. current was subjected to a rotational stress wave that travelled along the wire when a voltage pulse was applied to a short coil around the wire. The wave was observed in the voltage output from another coil placed some distance along the wire. Actually, two waves were observed, first a compression wave, which was expected, followed by the unexpected, slower travelling, torsional wave.

Batteau, Flanagan and Yang have made a number of experiments with these wires supported by a contract with N.O.T.S. It has been found that the torsional wave provides a convenient information carrier that allows for adjustable delay times, providing a device which could be of considerable use in information processing problems of interest in other research being conducted here. (I).

The writers have attempted to develop a model for the delay line from which they could derive a relationship between the input and output voltages, described in this report. These results now provide a basis for experiments to determine their validity, and a set of hypotheses to be examined by study of relevant literature. These next steps should be interesting, because having just looked at one probably relevant paper on the "Wiedemann effect",⁽²⁾ it appears that at least one of our hypotheses, that relating to the cause of twisting, may need drastic revision.

II. Quasi-static Maxwell Equations for Electro-Mechanical System

The input of the delay line system shown was to have an unsteady current to the coil. The impedance of the coil was mainly of inductive type. The current in the coil may also be related to the magnetic field surrounding the coil. The magnetic flux \bar{B} , induced inside the nickel wire interacted with the steady current supplied through the nickel wire. The result of the interaction, $\bar{J} \times \bar{B}$, may be the origin of the stress waves. This will be continued in a later section.



For any unsteady magnetic flux \bar{B} , there exists in general an electric field \bar{E} . The relationship of \bar{B} and \bar{E} follows the Maxwell Equations (Appendix A). Since the exact solutions of the Maxwell equations are complicated and involved, approximations are needed.

For the majority of electro-mechanical systems, the mechanical velocities and operating frequencies are low enough so that the electro-magnetic part of the system can be treated as almost static (quasi-static). This is allowable since the sonic velocities in a solid are usually less than 8×10^3 meters/sec. and these sonic velocities are very much less than the velocity of light (3×10^8 meters/sec.) The speed of electro-magnetic waves in material may be one order of magnitude smaller.

As in any approximation, its validity depends on the detailed nature of the system to be analyzed. We define our system as a magnetic system,

in which the primary excitation is the free current density J , and the primary field is the magnetic field. For the quasi/static case, the Maxwell equations become

$$\oint_C \bar{H} \cdot d\bar{l} = \iint_S \bar{J} \cdot \bar{n} da$$

$$\oint_C \bar{B} \cdot \bar{n} da = 0$$

$$\oint_C \bar{J} \cdot \bar{n} da = 0$$

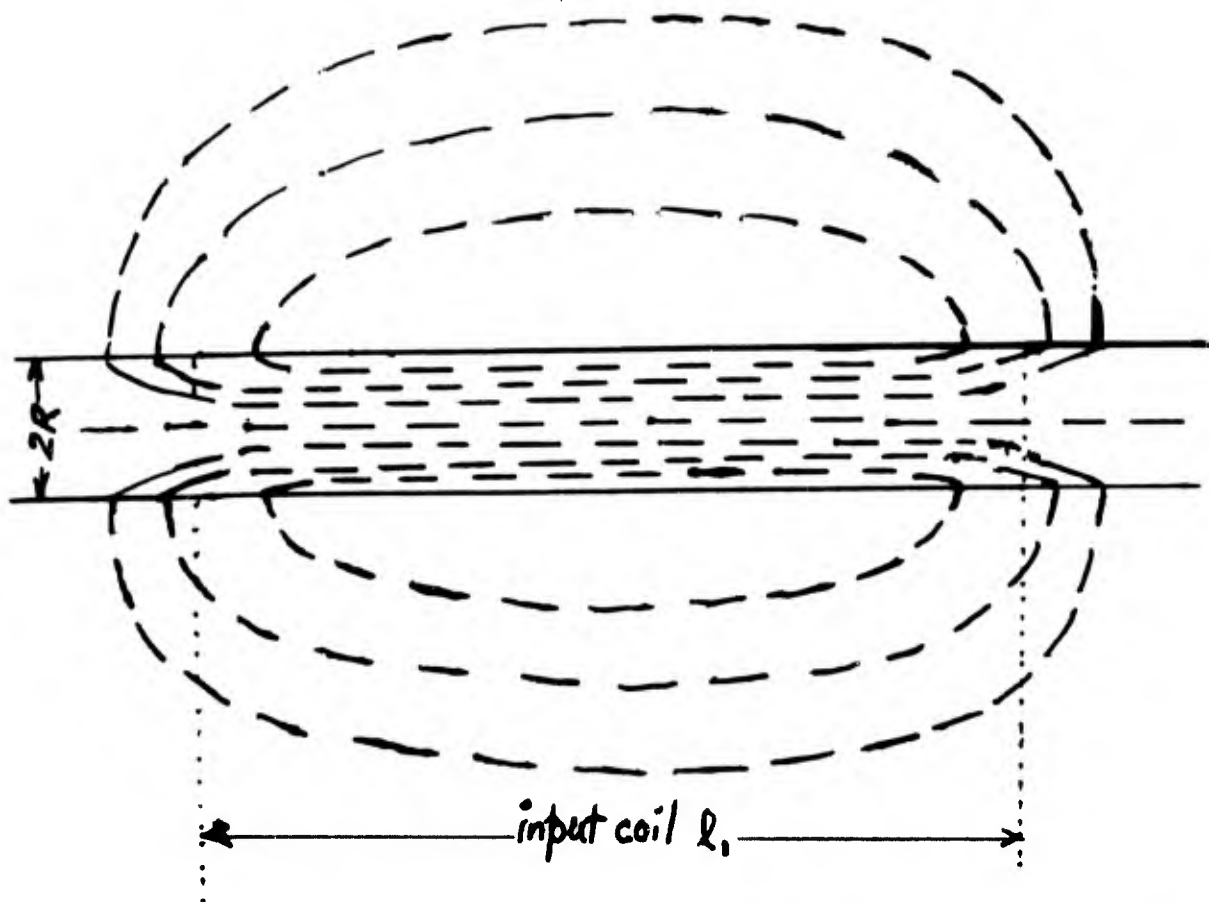
$$\bar{B} = \mu \bar{H}$$

These equations as well as boundary conditions will be used to determine the field function \bar{B} and in turn, the body forces which produce the mechanical distortions propagating as waves along the wire.

If the solution from the above quasi-static equations and the given boundary conditions is not adequate, a more accurate solution can be obtained by iteration. Substitute the quasi-static solution into the Maxwell equations and solve for the unknowns as additional quantities. This iteration can be carried out for any degree of accuracy.

III. Body-forces Due to the Magnetic input

Using the quasi-static equation, the magnetic flux (density) \bar{B} can be sketched as follows.



For the condition $l_1 \gg R$, the axial field density \bar{B}_a in the nickel wire will be uniform in the middle region of the coil. The radial components of the magnetic fluxes \bar{B}_r exist only near the two ends of the coil. The field is a function of time and varies with the input current in the coil. Since the nickel wire is rotationally symmetric in geometry, so too is the magnetic flux density \bar{B} .

The interaction of the conducting current I_0 with the two radial components of the magnetic fluxes may produce the rotational stress wave. The axial components may be responsible for the compressional stress wave. The body force \bar{F} in general will be [3];

$$\bar{F} = \iiint_V (\rho_c \bar{E} + \bar{J} \times \bar{B} - \frac{1}{2} H^2 \nabla \mu) dV$$

If a large steady state current density, $\bar{J}_{con.}$, is supplied to the nickel wire, the total current density \bar{J} will be the sum of the conducting $\bar{J}_{con.}$ and the magnetic current density $\bar{J}_{mag.}$ [4]. The induced eddy current density is neglected. For this study of the rotational stress wave, \bar{F} may be considered to

be $\bar{F} = \iiint_V \bar{J} \times \bar{B} dV$. Then, the torque \bar{T} , which produces the rotational displacement, $\theta(t)$, is $\bar{T} = \iiint_V (\bar{J} \times \bar{B}) \times \bar{F} dV$

IV. Torque and Angular Displacement

In the derivation of the torque expression (Appendix B), the sum of the steady conducting current and the steady magnetic current [4], both inside the nickel wire, will be substituted into the equation. The magnetic flux density, \bar{B} , will be the radial components only which exist near the two ends of coil. Then, the torque T can be related to the angular displacement θ in a linear manner for the nickel wire.

$$\theta = \frac{T l_1}{G_n \mathbb{I}}$$

Where \mathbb{I} is the second moment of area.

Finally, the angular displacement θ at any time and at any point along the nickel wire may be a function of $N_1, I_0, i(t), G_n$, and R, μ or

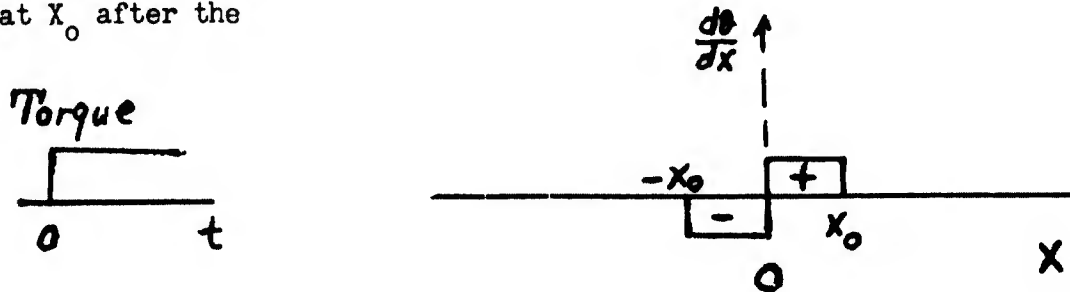
$$\theta = \frac{\mu(\mu+1) N_1 I_0 i(t)}{2 \pi G_n R^2}$$

[see Appendix B]

At a special condition, i.e., $i(t) = \text{constant}$ with respect to time, θ will be the displacement caused by two equal and opposite torques.

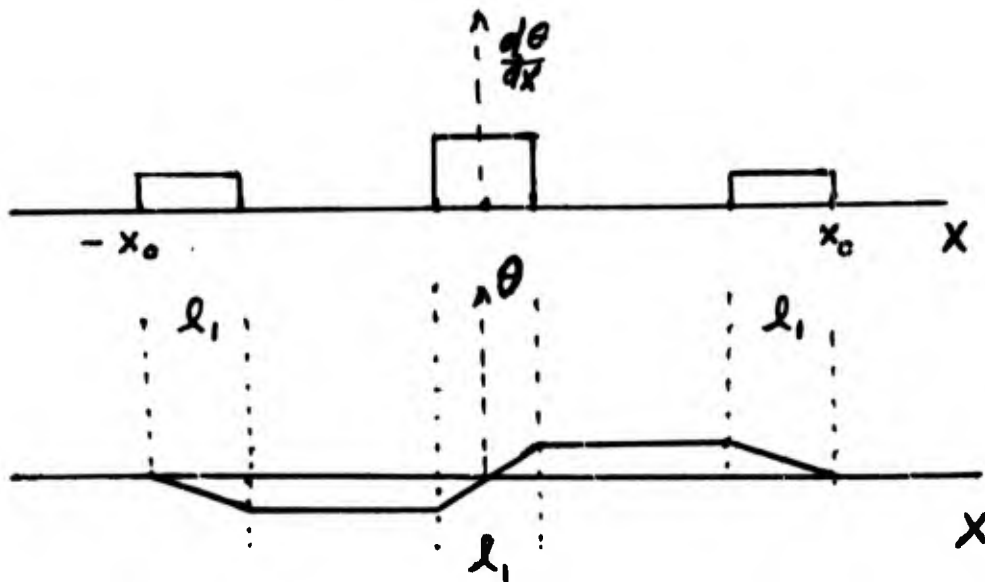
V. Stress Wave Propagation and Output Voltage

With a step function of the current $i(t)$, the two torques (twist) acting in the nickel at the region near the two ends of the input coil will be a step function too. If a single concentrated torque of step function acts at a point of the nickel wire, $X = 0$, the wave front will be at X_0 after the



time t_0 . The region (+) at the right of $X = 0$ will be considered as a positive angular strain, $\frac{d\theta}{dx} > 0$, while the region to the left of $X = 0$ will be the negative strain. $\frac{d\theta}{dx} < 0$ [5]

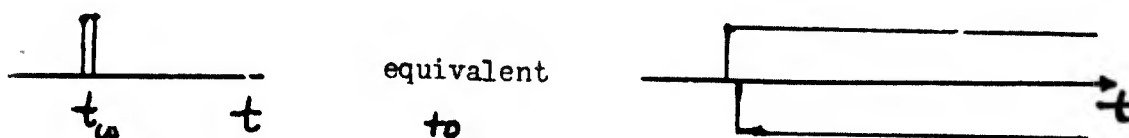
The result of adding two opposite torques for a step current will be shown:



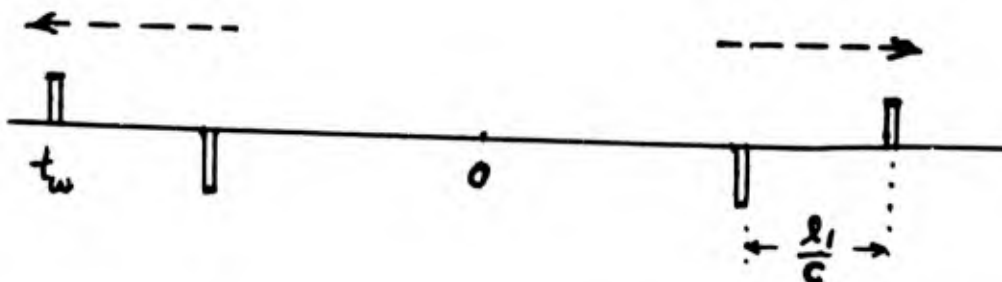
These diagrams will be valid if;

- a) the attenuation is zero
- b) the wave front is small compared to λ_1 , where the wave front is defined as the region at which the inertia effect is located.

The above discussion is the result of a step current $i(t)$ at the input coil. When a pulse current of width t_w is applied, the result will be the sum of two opposite and equal steps with a shift in time of t_w . Or



Then the stress pulses generated will be



A downstream pick-up coil will give a voltage reading due to the motion of the strained region. The following will describe briefly the mechanism of the inverse process.

The inverse coupling of stress waves and the magnetic flux changes may be modeled either as the inverse magnetostriction or as the displacement of the residual magnetism. The former one has been initially investigated by B. Langenecker [6]. The result of either concept will lead approximately to the following. As the strained regions (stress waves) propagate along the nickel wire, a magnetic flux moves with the stress waves. When the stress waves pass through the output coil, the change of the magnetic flux with time will be read out as a voltage output.

If the inverse magnetostriction model is adopted, then the magnetic flux can be calculated as a function of the stress wave,

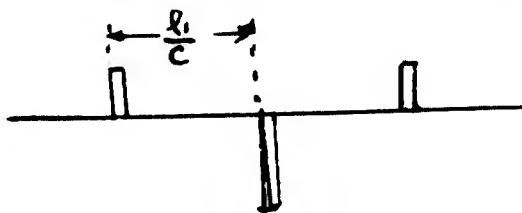
$$\begin{aligned} \Phi &\sim \int_0^R \frac{d\theta}{dx} r 2\pi r dr \\ &= g \frac{d\theta}{dx} R^3 \doteq g \frac{\theta}{l_1} R^3 \end{aligned}$$

g is constant.

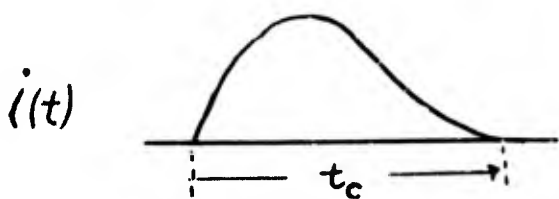
In general, the output voltage at the pick-up coil will be

$$V_2 = \frac{d\Phi}{dt}$$

Therefore, the voltage will be a function of the stress waves and the length of the output coil. Using the stress pulses generated by the pulse current input, previously discussed, and the length of the output coil l_2 equal to that of the input coil l_1 , the voltage pulses are



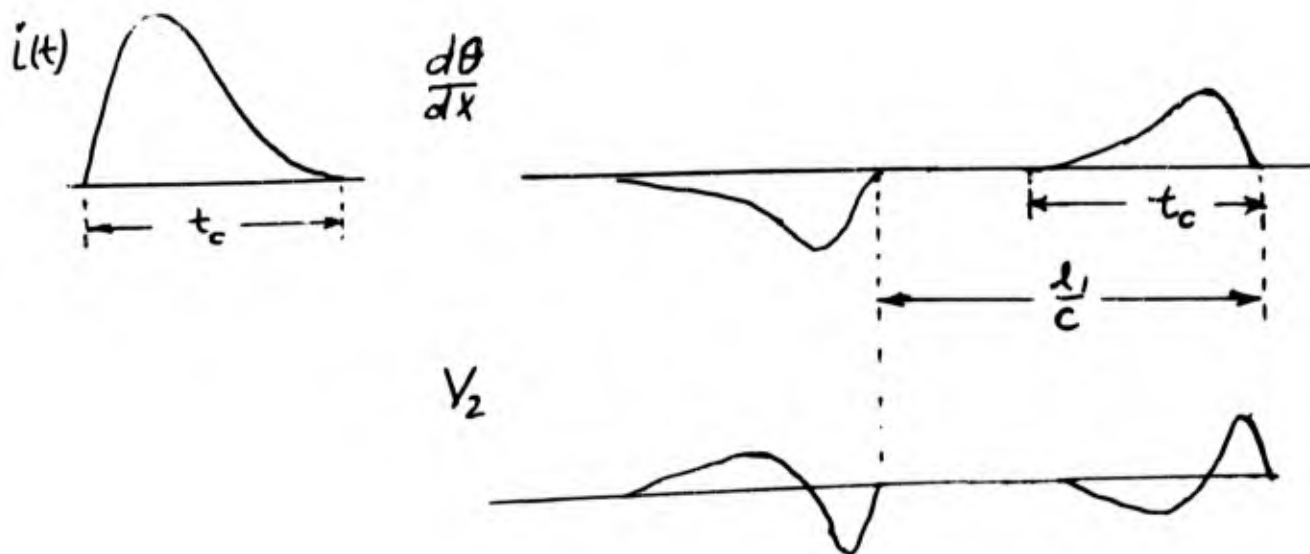
Using the superposition rule, the stress waves $\frac{d\theta}{dx}$ and the output voltage (V_2) of any given input current can be sketched: As follows.



V_2 for $l_1 = l_2$

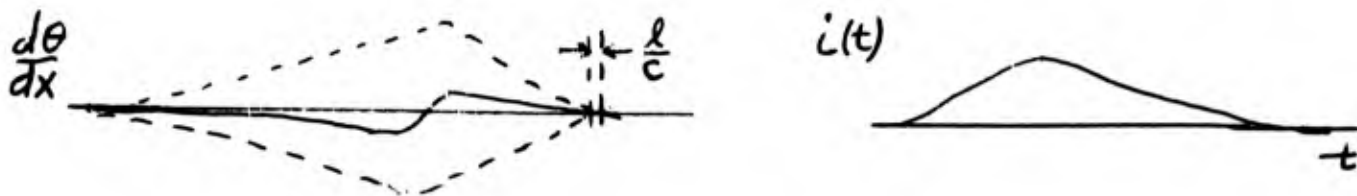


Under a different condition $\frac{l_1}{c} > t_c$ and $t_c > \frac{l_2}{c}$, the result for a given $i(t)$ is as shown below.



In the above two special cases; e.g. i) $\frac{l_1}{c} = \frac{l_2}{c}$; ii) $\frac{l_1}{c} > t_c > \frac{l_2}{c}$, the voltage outputs V_2 , were easily determined by sketching. However, under the following condition, V_2 can be written in a close form.

If the curve of the strain wave $\frac{d\theta}{dx}$, is reasonably smooth compared to the time of $\frac{l_1}{c}$, the voltage V_2 can be put into a closed form as illustrated.



Letting $\frac{l_1}{c} = \frac{l_2}{c} = \frac{l}{c}$, then



The pattern of the magnetic flux is similar to that of the strain wave. The magnetic flux traveling with the strain wave is the difference of two functions. Both are of the same form as the current input function, but one is delayed by $\frac{l_1}{c}$ with respect to the other. Since $\frac{l_2}{c}$ is negligible, the voltage can be simply equal to the derivative of the magnetic flux curve.

Or
$$V_2 = N_2 \frac{d\phi}{dt}$$

$$V_2(t') = \frac{N_2 g R^3 \mu (\mu + 1) N_1 I_0}{2\pi l_1 G_n R^2} \left[\left. \frac{di}{dt} \right|_t - \left. \frac{di}{dt} \right|_{t+\Delta t} \right]$$

The time t' is considered to start when the strain wave reaches the output coil. Δt is equal to $\frac{l_1}{c}$. Expanding the $\left. \frac{di}{dt} \right|_{t+\Delta t}$ in terms of Taylor series and neglecting higher order terms,

$$V_2(t) = \frac{g N_1 N_2 \mu (\mu + 1) I_0 R P^{\frac{1}{2}}}{G_n^{3/2}} \frac{d^2 i}{dt^2}$$

The current $i(t)$ at the input coil can be expressed as $i(t) = V_1(t) / Z$

For an inductive coil, the impedance Z is mainly $L \frac{\partial}{\partial t}$

Where
$$L = \frac{\mu N_1^2 \pi R^2}{\chi_1}$$

Hence, by substitution,

$$V_2(t') = \frac{g N_2 (\mu + 1) I_0 P^{\frac{1}{2}} l_1}{2\pi^2 N_1 R G^{3/2}} \frac{dV_1(t)}{dt}$$

$t' = t - D.t$ $D.t = \text{delay time}$

V. CONCLUSION

A model was proposed for the mechanism of the origin of the rotational stress wave in the nickel wire when an unsteady voltage was supplied to a coil around the wire and a steady state current was supplied to the wire. Further study is needed to examine the validity of the assumptions made. However, the relationship of the voltage V_1 at the input coil and the voltage V_2 at the output coil was derived as

$$V_2 = \frac{g N_2 (\mu + 1) I_0 \rho^{\frac{1}{2}} l_1}{2\pi^2 R N_1 G_n^{3/2}} \frac{dV_1}{dt}$$

if and only if

- (1) the electro-mechanical system is quasi-static;
- (2) the effect of the eddy current in nickel is small;
- (3) the length of the input coil is larger than the diameter of the nickel wire;
- (4) the radial component of the magnetic flux density, $B_r(r, x, t)$ can be separable; e.g., $B_r(r, x, t) = f(r) g(x) h(t)$, near the two ends of the input coil;
- (5) the wave front at which the inertia effect is located is small compared to the length of the coil;
- (6) the inverse coupling of the stress wave and the magnetic flux change is linear. The mechanism may be modeled either as the inverse magnetostriction or as the displacement of the residual magnetism;
- (7) the Maxwell equations hold;
- (8) the curve of the input current function $i(t)$ is reasonably smooth;
- (9) in the Taylor expansion of $\frac{di}{dt}$, $\left(\frac{l}{c}\right)^2 \frac{d^3 i}{dt^3} \ll \frac{l}{c} \frac{d^2 i}{dt^2}$.

APPENDIX A: MAXWELL EQUATIONS FOR A ELECTRO-MAGNETIC SYSTEM

For a continuum model, the following are assumed to hold:

1. Conservation of Charges

$$\oint \vec{J} \cdot \vec{n} \, da = - \frac{d}{dt} \iiint_V \rho_c \, d\tau$$

where

\vec{n} = outward normal to the surface

\vec{J} = current density in Amperes/m²

ρ_c = charge density in Coulombs/m³

2. Lorentz Force

$$\vec{F} = \rho_c \vec{E} + \vec{J} \times \vec{B}$$

3. Faraday's Law

$$\oint_C \vec{E} \cdot d\vec{l} = - \frac{d}{dt} \iint_S \vec{B} \cdot \vec{n} \, da$$

4. Ampere's Law

$$\oint_C \vec{H} \cdot d\vec{l} = \iint_S \vec{J} \cdot \vec{n} \, da + \frac{d}{dt} \iint_S \vec{D} \cdot \vec{n} \, da$$

5. Auxiliary Relations

$$\vec{B} = \mu \vec{H}$$

$$\oint_S \vec{B} \cdot \vec{n} \, da = 0$$

$$\vec{D} = \epsilon \vec{E}$$

$$\oint_S \vec{D} \cdot \vec{n} \, da = \iiint_V \rho_c \, d\tau$$

$$\vec{J} = \sigma \vec{E}$$

APPENDIX B: DERIVATION OF ANGULAR DISPLACEMENT, $\theta(t)$

In section III, the torque which produced the angular displacement (rotational) was expressed as

$$\bar{T}(t) = \iiint (\bar{J} \times \bar{B}) \times \bar{r} \, dV \quad (1)$$

Inside the volume integral, the value \bar{J} will be a sum of a conducting current density \bar{J}_{con} and a magnetic current density \bar{J}_{mag} . [4] When a current $I_0 (= J_{con} \pi R^2)$ is supplied into the nickel wire of diameter $2R$, a very large magnetic field, \bar{B} , is induced inside the nickel. On the other hand, with the same current I_0 in a copper wire of the same diameter, $2R$, a rather small magnetic field exists in the copper. $\bar{B} = \mu \bar{H}$. For the Nickel case, $\mu = 500$; while $\mu = 1$ for copper. The large \bar{B} in the ferromagnetic material (nickel) can be explained by introducing a new vector \bar{M}

$$\bar{M} = \bar{B} - \bar{H} \quad (a)$$

$$\bar{J}_{con} = \nabla \times \bar{H} \quad (b)$$

$$\bar{J}_{mag} = \nabla \times \bar{M} \quad (c)$$

Where \bar{M} is the vector of the permanent magnetism in the ferromagnetic material.

$$\text{Since } \bar{J}_{con} = \frac{I_0}{\pi R^2} \hat{r}; \quad \bar{H} = \frac{\bar{J}_{con} \times \bar{r}}{2}$$

$$\text{Hence } \bar{J} = \bar{J}_{con} + \bar{J}_{mag} = \frac{\mu + 1}{2} \frac{I_0}{\pi R^2} \hat{r} \quad (2) \text{ by combining (a), (b), and (c),}$$

(2)

The direction of \bar{J} is parallel to that of the conducting one. It is uniform across the whole cross-sectional area in the nickel, except at the surface where singularity occurs. The magnitude of the (opposite to \bar{J}) surface current would be equal to the product of the magnetic current density and the cross-sectional area. The net current should be equal to the conducting one.

Before substituting J into equation (1), the magnetic flux density \bar{B} should be discussed. As in Section III, the part of the magnetic field which will be used is the two radial components, B_r , at the regions near the two ends of the coil. Thus, in evaluating the torque at the end of the coil,

From (1) and (2)

$$\begin{aligned} T &= \int_0^R \int_0^R \frac{\mu+1}{2} \frac{I_0}{\pi R^2} B_r(r, x, t) 2\pi r \cdot r dr dx \\ &= (\mu+1) \frac{I_0 \pi}{\pi R^2} \int_0^R \int_0^R B_r(r, x, t) r^2 dr dx \end{aligned} \quad (d)$$

If $B_r = f(r) g(x) h(t)$ and

Since $\int f(r) g(x) h(t) dx = \frac{\mu}{l_1} N_1 i(t) r$

Equation (d) becomes

$$\begin{aligned} T &= \frac{(\mu+1) I_0}{R^2} \int_0^R r^2 dr \frac{\mu}{l_1} N_1 i(t) r \\ &= \frac{(\mu+1) \mu I_0 N_1 i(t) R^2}{4 l_1} \end{aligned} \quad (e)$$

Then, the angular displacement θ is $\frac{T l_1}{G_n \Pi}$

$\Pi \equiv \int_0^R r^2 2\pi r dr = \frac{\pi R^4}{2}$, the second moment of area, meter⁴

G_n = shear modulus of nickel in Newtons'/m²

Or
$$\theta(t) = \frac{\mu(\mu+1) N_1 I_0 i(t)}{2 \pi R^2 G_n} \quad \text{for nickel}$$

For copper

$$\theta(t) \sim \frac{N_1 I_0 i(t)}{R^2 G_c}$$

If the nickel line is replaced by a copper wire of a diameter $2R$.

G_c = shear modulus of copper

REFERENCE

1. Batteau, D. W. and G. P. Flanagan., "A Study of Acoustical Multi-Path System, Section IV, Delay Line" 1 June 1966 Final Report: Contract No. RN 494 (00) U.S. Navy Office of Naval Reseach.
2. Smith, R. and K. J. Overshott, "The Wiedemann Effect: A theoretical and experimental comparison". Brit. J. Appl. Phys. 16, 1965.
3. Straton, "Electro-Magnetic Theory"., p 158.
4. Feynman, Leighton, Sands, "The Feynman Lectures on Physics", Vol. 2.
5. Lamb, "Hydrodynamics"
6. Langenecker, B., "Inverse Magnetostriction Effect of Ultrasonic Stress Waves in Steel", J. Acous. Soc. Am., Vol. 38,pp 234-238, August, 1965.

THREE DIMENSIONAL STRESS -STRAIN -MAGNETIC FIELD RELATIONS
FOR AN ISOTROPIC FERROMAGNETIC MATERIAL

by Philip Yang
Mechanical Engineering Department
Tufts University
9 November 1966

(A paper submitted to the A.S.M.E.-Applied Mechnics
Division)

CONTENTS

NOMENCLATURE

I. INTRODUCTION

2. ANALYSIS

2.1 Elastic Part of the System

2.1.1 General Stress - Strain Relation

2.1.2 Elastic Energy

2.1.3 Stress - Invariant Method

2.2 Magnetic Energy, U_m

2.3 Coupling Between the Elastic and the Magnetic Energies

2.4 General Stress- Strain and Magnetic Field Equations

2.5 Determinations of Material Constants

2.5.1 One Dimensional Joule Effect

2.5.2 Two Dimensional Wiedemann Effect

3. CONCLUSION

ACKNOWLEDGEMENTS

REFERENCES

FIGURES 1, 2

APPENDIXES A AND B

NOMENCLATURE

- E - Young's modulus pound/meter²
 ν - Poisson's ratio
 λ - Lamé' constant pound/meter²
 G - rigidity modulus (shear modulus) pound/meter²
 ϵ_{ij} - strain component directed along the i axis and acted on the
 face whose unit normal is along the j axis. meter/meter
 $i = 1, 2, 3; j = 1, 2, 3$ or x, y, z
 $\epsilon_{11} = \epsilon_1$
 e_{kk} - $e_{11} + e_{22} + e_{33}$
 σ_{ij} - similar stress component pound/meter²
 C_k - constant coefficient $k = 1, 2, 3$
 W - work, pound-meter
 U_e - elastic energy, pound-meter
 U_m - magnetic energy, Joule
 h_k - magnetic component along the k th axis. $k = 1, 2, 3$, or x, y, z Gauss
 ($10^3/4\pi$ Ampere/meter) (Oe)
 θ - angle of twist over the entire length / , rad
 μ - permeability of material

I. INTRODUCTION

Ferromagnetic material such as nickel, iron, cobalt, and their alloys deform dimensionally when a magnetic field is applied to them. A cylindrical nickel rod decreases in length when an axial magnetic field is applied. Hence, nickel is called magnetostriction negative. On the other hand, an iron rod expands or increases in length with an applied magnetic field and is called magnetostriction positive. The above physical phenomena were first noted by Joule and are referred to as the Joule Effect. (1,2,3,4)

A twist in the rod was also observed by Wiedemann when a two-dimensional magnetic field was applied, an axial component and a tangential component, to the rod. The direction of the twist depended upon the property of the material (either magnetostriction positive or negative) and the orientations of the applied magnetic field. (5)

These effects were used in systems such as analog or digital computers as delay lines. (6,7,8,9,10) The Wiedemann Effect has been used extensively in the recent work (11), since in the torsional mode, the delay time is longer for the same length of the delay line and the dispersion of the signal waves is negligible.

The magnitude of the twist in a rod is a function of the two components of the magnetic field, and the properties of the material. (5) This functional relationship has not been investigated well. For the lack of the three dimensional relationship of the stress-strain and the applied magnetic field, the description of the two dimensional twist made in the recent work (11) seemed inadequate. This study is aimed to derive a set of three dimensional equations by using the Thermodynamic Laws, the scalar and vector properties of the energy and the stress, and the symmetry of the material. We limit our argument to the case of negligible hysteresis losses of both the magnetic energy and the mechanical energy. It is also under the isothermal (constant temperature) and adiabatic (no heat transfer) conditions.

2. ANALYSIS

Both the Joule and Wiedemann Effects are the result of the coupling between the elastic energy and the magnetic energy. The arguments or the logic to establish the needed coupling energy are what we are going after. If the development of the simple elastic energy uncoupled from the magnetic field contains to a certain extent what we want, then we ought to consider the elastic part first.

2.1 The Elastic Part of the System

2.1.1. The General Stress-Strain Relation

The general equations have been known to us for many years. (12) For an elastic, isotropic medium, the linear stress-strain equations contain only two elastic constants, either E and ν ; λ and G or any two combinations of the four. (Appendix A).

$$E_{ij} = \frac{1}{E} [\sigma_{ij}(1+\nu) - \nu(\sigma_{kk})] \quad i = j$$

$$= \frac{2(1+\nu)}{E} \sigma_{ij} \quad i \neq j$$

The principal axes of stress coincides with that of strain. The stress invariants I_1 , I_2 and I_3 are

$$I_1 = \sigma_{xx} + \sigma_{yy} + \sigma_{zz}$$

$$I_2 = \sigma_{xx}\sigma_{yy} + \sigma_{yy}\sigma_{zz} + \sigma_{zz}\sigma_{xx} - \sigma_{xy}^2 - \sigma_{yz}^2 - \sigma_{zx}^2$$

$$I_3 = \begin{vmatrix} \sigma_{xx} & \sigma_{xy} & \sigma_{xz} \\ \sigma_{yx} & \sigma_{yy} & \sigma_{yz} \\ \sigma_{zx} & \sigma_{zy} & \sigma_{zz} \end{vmatrix}$$

These invariants may be used in the energy expression in later sections.

2.1.2. Elastic Energy

From the First Law of Thermodynamics, the adiabatic work is equal to the energy and it is a point function or an exact differential. The elastic energy may also be shown as a function of the stresses and the two elastic constants (Appendix B)

$$U_e = W = \frac{1}{2E} (\sigma_{xx}^2 + \sigma_{yy}^2 + \sigma_{zz}^2) - \frac{\nu}{E} (\sigma_{xx}\sigma_{yy} + \sigma_{yy}\sigma_{zz} + \sigma_{zz}\sigma_{xx}) + \frac{(1+\nu)}{E} (\sigma_{xy}^2 + \sigma_{yz}^2 + \sigma_{zx}^2) \quad 2.1.2 (a)$$

The elastic energy W is a scalar quantity. Any scalar quantity is independent of the choice of the coordinate system. While the stress σ_{ij} is a tensor quantity and its value in general is dependent on the coordinate axes, only the invariants of the stress tensor, which have the same properties as the energy, can be related to the energy. Hence, the elastic energy may be expressed in terms of the stress invariants, the equation 2.1.2 (a) can be put as

$$W = \frac{1}{2E} I_1^2 - \frac{(1+\nu)}{E} I_2$$

$$I_1 = \sigma_{xx} + \sigma_{yy} + \sigma_{zz}$$

$$I_2 = \sigma_x \sigma_y + \sigma_y \sigma_z + \sigma_z \sigma_x - \sigma_{xy}^2 - \sigma_{yz}^2 - \sigma_{zx}^2$$

Actually, the elastic energy, W , may be derived directly in the next section by using the properties of scalar and vector quantities, and the invariants of the stress tensor. These properties will also be used in deriving the coupling energy between the elastic and magnetic energies.

2.1.3. Stress - Invariant Method.

The elastic energy can be expressed as a power series of these stress invariants.

$$W = c_1 (\sigma_{11} + \sigma_{22} + \sigma_{33}) + c_2 (\sigma_{11}\sigma_{22} + \sigma_{22}\sigma_{33} + \sigma_{33}\sigma_{11} - \sigma_{12}^2 - \sigma_{23}^2 - \sigma_{31}^2) + c_3 (\sigma_{11} + \sigma_{22} + \sigma_{33})^2 + \dots$$

If the argument is limited to the case of small variations, i.e., $(\frac{\sigma}{E})^3 \ll (\frac{\sigma}{E})^2$, then the third and higher orders of stress terms can be neglected in the above equation. Since the stress is a vector quantity, $C_1 = 0$; and since the elastic energy \underline{W} is a point function, the strain is

$$\begin{aligned} \epsilon_{ij} &= \frac{\partial W}{\partial \sigma_{ij}} = C_2 (\sigma_{kk} - \sigma_{ij}) + 2C_3 (\sigma_{kk}) & i = j \\ &= -2C_2 \sigma_{ij} & i \neq j \end{aligned}$$

By comparing with the stress-strain equations in Section 2.1.1., we have

$$C_2 = -\frac{(1+\nu)}{E} \quad \text{and} \quad C_3 = \frac{1}{2E}. \quad \text{Hence, the elastic energy } \underline{W} \text{ is}$$

$$W = \frac{1}{2E} I_1^2 - \frac{(1+\nu)}{E} I_2$$

Similarly, the magnetic energy and the coupling energy may also be made available by this invariant technique.

2.2 Magnetic Energy U_m

$$U_m = \frac{\mu}{2} h_k h_k \qquad B_k = \frac{\partial U_m}{\partial h_k} = \mu h_k$$

2.3 Coupling Between the Elastic and the Magnetic Energies.

The magnetic effect on the elastic energy is similar to that of the thermal effect. The stress-strain field is set up by the change of either the magnetic field or the thermal field (the temperature field). But the analogy is not complete, since the magnetic field equations should be different from the stress-strain temperature equations.

Considering all the possible combinations of both the magnetic and stress invariants,

$$\begin{aligned}
 U_c = & C_{11}\sigma_{11}h_1 + C_{22}\sigma_{22}h_2 + C_{33}\sigma_{33}h_3 + (\sigma_{kk})[C_2h_{kk} + C_3h_k h_k] \\
 & + C_4(\sigma_{11}h_1^2 + \sigma_{22}h_2^2 + \sigma_{33}h_3^2) + C_5(\sigma_{12}h_1h_2 + \sigma_{23}h_2h_3 + \sigma_{31}h_3h_1) \\
 & + C_6(\sigma_{kk})^2[(h_{kk})^2 + \dots]
 \end{aligned}$$

For small variations again, $C_6 = 0$. Since the coupling energy, U_c , is also independent of the choice of the coordinate system, thus the naming of 1, 2, and 3 is arbitrary, $C_{11} = C_{22} = C_{33} = C_1$. Hence, the coupling energy is simplified to the following form.

$$\begin{aligned}
 U_c = & C_1(\sigma_{11}h_1 + \sigma_{22}h_2 + \sigma_{33}h_3) + (\sigma_1 + \sigma_2 + \sigma_3)[C_2(h_1 + h_2 + h_3) + C_3(h_1^2 + h_2^2 + h_3^2)] \\
 & + C_4(\sigma_1h_1^2 + \sigma_2h_2^2 + \sigma_3h_3^2) \\
 & + C_5(\sigma_{12}h_1h_2 + \sigma_{23}h_2h_3 + \sigma_{31}h_3h_1)
 \end{aligned}$$

The sum of the coupling energy and the elastic energy will be used to derive the general equations in the next section.

2.4. The General Stress-Strain and Magnetic Field Equations.

$$\epsilon_{ij} = \frac{\partial U}{\partial \sigma_{ij}}$$

$$U = U_c + U_e$$

$$\epsilon_{11} = \frac{1}{E}[\sigma_{11}(1+\nu) - \nu(\sigma_{kk})] + C_1h_1 + C_2h_{kk} + C_3h_k h_k + C_4h_1^2$$

$$\epsilon_{22} = \frac{1}{E}[\sigma_{22}(1+\nu) - \nu(\sigma_{kk})] + C_1h_2 + C_2h_{kk} + C_3h_k h_k + C_4h_2^2$$

$$\epsilon_{33} = \frac{1}{E}[\sigma_{33}(1+\nu) - \nu(\sigma_{kk})] + C_1h_3 + C_2h_{kk} + C_3h_k h_k + C_4h_3^2$$

$$\epsilon_{12} = \frac{2(1+\nu)}{E}\sigma_{12} + C_5h_1h_2$$

$$\epsilon_{23} = \frac{2(1+\nu)}{E} \sigma_{23} + C_5 h_2 h_3$$

$$\epsilon_{31} = \frac{2(1+\nu)}{E} \sigma_{31} + C_5 h_3 h_1$$

$C_1, C_2, C_3, C_4,$ and C_5 are constants of material properties. This set of general equations is different from those of the stress-strain and temperature equations as mentioned earlier.

In Section 2.1, it was mentioned that the principal axes of stress always coincide with those of strain. It may be shown in the following that the principal axes of stress in general do not coincide with the axes along which the components of the magnetic field are directed. If we use the principal axes of stress as the coordinate system through transformation, then the shearing stresses (shearing strains) are zero in those axes. Actually, that is the definition. If we apply the components of the magnetic field along those axes, and if these axes coincide with the principal axes of stress produced, then the general case would rule out any twist. This contradicts the Wiedemann Effect. That is, the principal axes of stress do not coincide with $r - \theta - z$ cylindrical coordinates when the two dimensional magnetic fields, h_θ and h_z , are applied to the simple cylindrical rod.

2.5. Determinations of Material Constants.

The constants $C_1, C_2, C_3, C_4,$ and C_5 in Section 2.4 can be correlated with the available experimental data in the literature (5, 13, 14, 17) for the most useful material. The data consisted of two groups, i.e., the

Joule Effect and the Wiedemann Effect.

2.5.1. One Dimensional Joule Effect.

If the cylindrical coordinate system (r, θ, z) is used, the applied magnetic field is $h_r = h_\theta = 0$, and $h_z = H_0$. Since the rod is free to deform, $\sigma_{1j} = 0$. Then, the equations in Section 2.4 can be simplified as

$$e_r = C_2 H_0 + C_3 H_0^2$$

$$e_\theta = C_2 H_0 + C_3 H_0^2$$

$$e_z = (C_1 + C_2) H_0 + (C_3 + C_4) H_0^2$$

$$e_{r\theta} = e_{\theta z} = e_{zr} = 0$$

Correlating the above equations with the curves in Figure 1, we obtain the following results. The unit of C_1 is meter/meter gauss and that of C_2 meter/meter gauss². ν_p is the Poisson's ratio of 45 Permalloy.

	C_1	C_2	C_3	C_4	
Material					
nickel	-3.9	+1.2	-0.034	+0.11	
iron	+0.43	-0.12	+0.01	-0.034	
cobalt	0	0	0	0	
45 Permalloy	$\frac{53}{30}$	$-\frac{53}{30} \nu_p$	$+\frac{7}{150} \nu_p$	$-\frac{7}{150}$	($H_0 \leq 40$ gauss)

2.5.2. Two Dimensional Wiedemann Effect

Similar to the Joule Effect, the angle of twist, θ , over the rod length l , can be expressed as a function of the magnetic field as follows. From the equation of Section 2.4., $e_{\theta z} = C_5 H_0 H_z$; $e_{\theta z} = r \theta / l$. (18).

Since $H_r = 0$, $e_{r\theta} = e_{zr} = 0$

Hence, $\frac{\theta}{l} = C_5 \frac{H_0 H_z}{r}$

C_5 is not a simple constant (5,13, 14). A typical case of the twist θ vs H_0 at constant H_z or vs H_z at constant H_0 is given in Figure 2. Figure 2 shows that C_5 depends very much upon the magnitude of the field, H_0 and H_z , as well as upon the properties of the material. From Figure 2, $C_5 = 0.14 \text{ sec/gauss}^2$, using the factor of 4.85×10^{-6} to convert radian to sec. The twists for iron, carbon steel and alfes (13% λ_1 -Fe) are different in sign from those for nickel and cobalt.

3. CONCLUSION

9

The three dimensional stress-strain-magnetic field equations were derived for the isotropic ferromagnetic material.

$$\begin{aligned} \epsilon_{ij} &= \frac{1}{E} [\sigma_{ij} (1 + \nu) - \nu (\sigma_{kk})] + C_1 h_i \\ &\quad + C_2 h_{kk} + C_3 h_k h_k + C_4 h_i^2 \quad i=j \\ \epsilon_{ij} &= \frac{2(1+\nu)}{E} \sigma_{ij} + C_5 h_i h_j \quad i \neq j \end{aligned}$$

The coupling constants of material, C's, were determined. This set of equations applies very well to both the Joule Effect and the Wiedemann Effect as expected.

The principal axes of stress (strain) do not in general coincide with the axes along which the components of the magnetic field are directed.

REFERENCES

- (1) Joule, J. P. "On the Effects of Magnetism upon the Dimensions of Iron and Steel Bars" *Phil. Magazine III*, Vol. 30, p.76 (1847)
- (2) Barret, W. F. "On the Alternations in the Dimensions of the Magnetic Metals by Act of Magnetization" *Nature* 26, p. 585 (1882)
- (3) Mason, W. P. "Piezoelectric Crystals and their Applications to Ultrasonics" D. Van Nostrand Co., Inc. Ch. 4,5 (1950)
- (4) Katz, H. W. "Solid State Magnetic and Dielectric Devices" John Wiley and Sons, Chapter 3 (1959)
- (5) S. R. Williams "A Study of the Joule and Wiedemann Magnetostrictive Effects in Steel Tubes" *Physics Review* 32, p. 281, (1911)
- (6) Bradburd, E. M. "Magnetostrictive Delay Line" *Electrical Communication*, 24:46 (March 1951)
- (7) Epstein, H., and Stram, O. "Magnetostrictive Sonic Delay Line" *Review of Scientific Instruments*, 24:231 (March 1953)
- (8) Robbins, R. C., and Millership, R. "Applications of Magnetostriction Delay Lines" *Proceedings of Symposium on Automatic Digital Computations, National Physical Lab., England*, p. 199 (March 1953)
- (9) DeBarr, A. E. "Digital Storage Using Ferromagnetic Materials" *The Elliott Journal, England*, 1:116 (May 1953)
- (10) Chaplin, G. B. B., Hayes, R. E., and Owens, A. R. "A Transistor Digital Fast Multiplier with Magnetostrictive Storage" *Proceedings IEE*, 102: 412 (July 1955)
- (11) Tzannes, N.S. "Joule and Wiedemann Effects - The Simultaneous Generation of Longitudinal and Torsional Stress Pulses in Magnetostrictive Materials" *IEE Transactions on Sonics and Ultrasonics* Vol. SU - 13 No. 2 (July 1966)

References - 2

- (12) Love, H. "Mathematical Theory of Elasticity" The MacMillan Co. (1932)
- (13) Pidgeon, H. A. "Magnetostriction With Special Reference to Pure Cobalt" Physics Review, 13: 209 (1919)
- (14) McCorkle, P. "Magnetostriction and Magnetoelectric Effects in Iron, Nickel and Cobalt" Physics Review 22: 271 (1923)
- (15) Zemansky "Heat and Thermodynamics" McGraw - Hill, Chapter 1, 2 (1937)
- (16) Hatsopoulos, G. N., and Keenan, J. H. "Thermodynamics" McGraw - Hill Chapter 3, 4, 5 (1965)
- (17) Bozorth "Ferromagnetism" Van Norstrand Co., Inc., N.Y. p. 631 (1951)
- (18) Crandall, S. H. and Dahl, N.C. "An Introduction to the Mechanics of Solids" McGraw- Hill p. 241 (1959)

ACKNOWLEDGMENT

The author is deeply indebted to Mrs. Julia C. Yang, his wife, Professor L. MacG. Trefethen and Professor D. W. Barreau. Mr. Thin Ng and Mr. Henry Wright are to be thanked for their helpful discussions, and Mrs. W. H. Carr for her typing.

Philip Yang
Department of Mechanical Engineering
Tufts University
Medford, Massachusetts

November 9, 1966

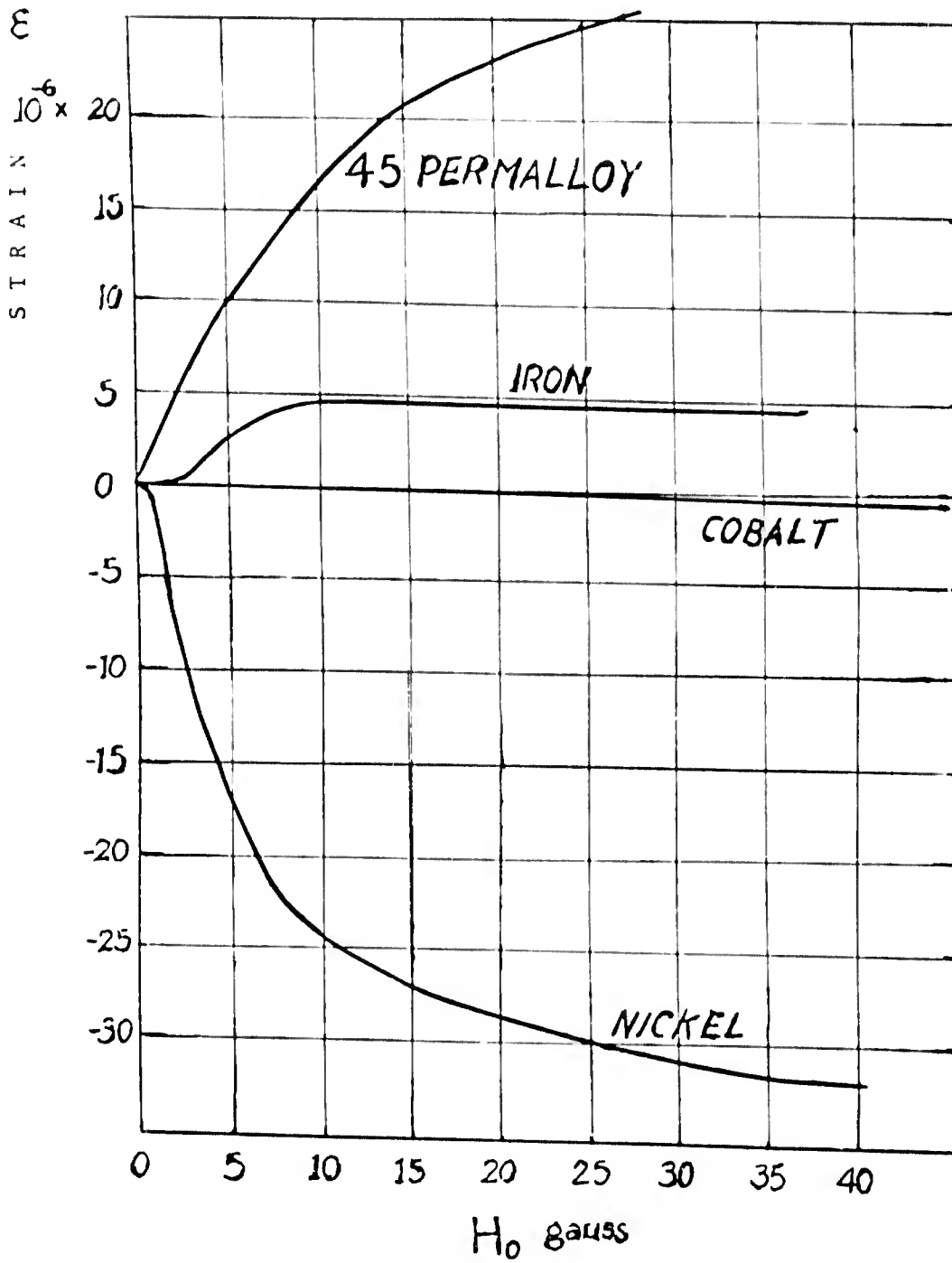
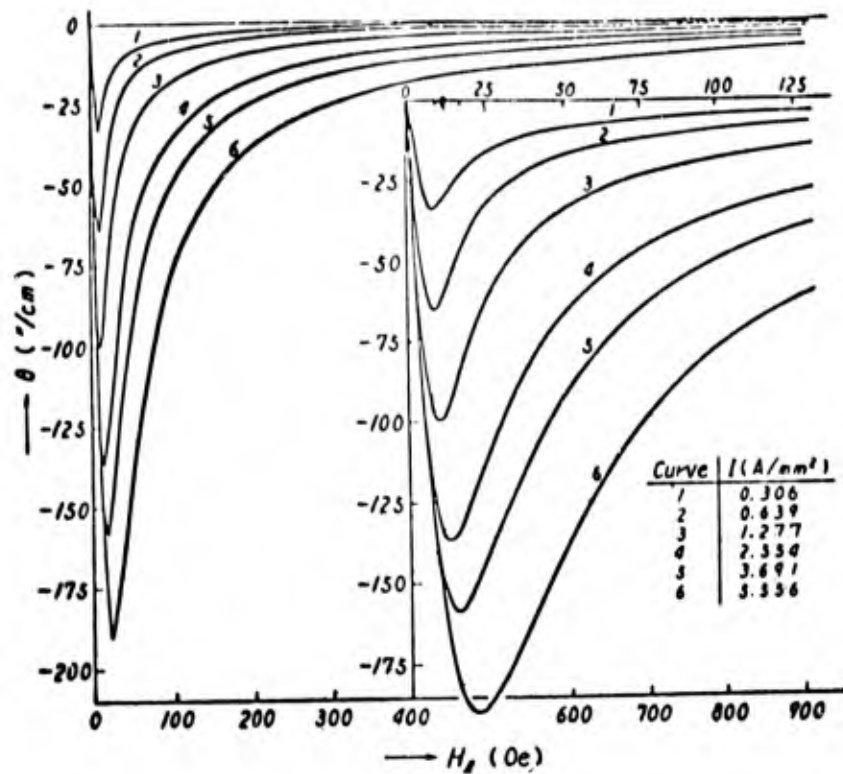
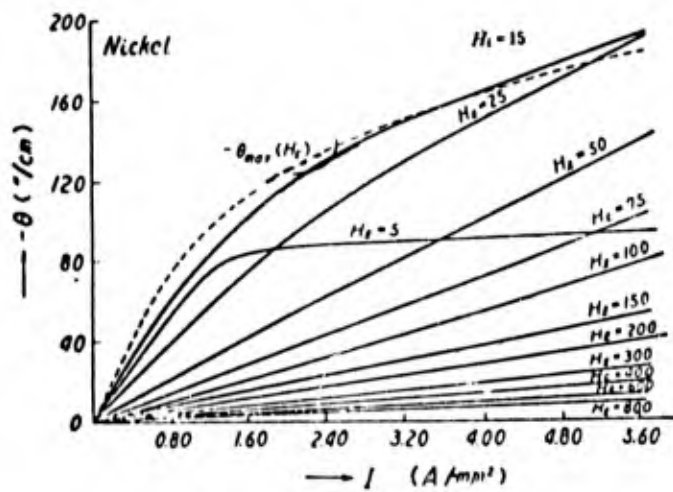


Fig. I Joule Effect of Strain vs Applied Magnetic Field (17)



(a)



(b)

Fig. 2 Wiedemann effect in a cylindrical rod specimen of nickel ($a = 0.0502$ cm, $L = 25.01$ cm; annealed at 800°C for 3 hours in a hydrogen stream) (Pitropi [3]). (a) $\theta(H_2)$ curves and (b) $\theta(I)$ curves.

APPENDIX A
THREE DIMENSIONAL STRESS- STRAIN RELATIONSHIP

In the most general form, each of the stress components is a linear function of the components of the strain tensor. That is,

$$\sigma_{11} = C_{11}e_1 + C_{12}e_2 + C_{13}e_3 + C_{14}e_{12} + C_{15}e_{23} + C_{16}e_{13}$$

$$\sigma_{23} = C_{61}e_1 + C_{62}e_2 + C_{63}e_3 + C_{64}e_{12} + C_{65}e_{23} + C_{66}e_{16}$$

In equilibrium, the stress tensor is symmetric; $\sigma_{12} = \sigma_{21}$.

So is the strain tensor. The thirty-six coefficients $C_{11} \dots C_{66}$ are material constants. If the elastic work is a point function, then

$$\frac{\partial^2 U}{\partial e_1 \partial e_2} = \frac{\partial^2 U}{\partial e_2 \partial e_1} \quad \text{or } C_{12} = C_{21}$$

The elastic constants C_{ij} are symmetrical too. Hence, due to the symmetry, the thirty-six constants are reduced to twenty-one. In other words, the anisotropic linearly elastic material has twenty-one elastic constants.

If we restrict our model to an isotropic medium, further simplification can be made. Fortunately, the isotropic model represents very well a large group of real materials. The following manipulations show that twenty-one anisotropic material constants can be reduced to only two constants for the isotropic case.

Using the symmetry, again, we can get:

$$C_{15} = C_{16} = C_{25} = C_{26} = C_{36} = C_{45} = C_{46} = 0$$

in the coordinate transformation

$$1 \rightarrow 1, 2 \rightarrow 2, 3 \rightarrow -3.$$

Similar transformation, $1 \rightarrow 1, 2 \rightarrow -2, 3 \rightarrow 3$, will give

$$C_{14} = C_{24} = C_{34} = C_{56} = 0. \quad \text{Since the naming of 1, 2, and 3 is arbitrary, } C_{11} = C_{22} = C_{33}, \quad C_{12} = C_{13} = C_{23}, \quad C_{44} = C_{55} + C_{66}$$

Then, the general stress-strain equations are

$$\sigma_1 = C_{11}e_1 + C_{12}(e_2 + e_3)$$

$$\sigma_2 = C_{12}(e_2 + e_3) + C_{11}e_2$$

$$\sigma_3 = C_{11}e_3 + C_{12}(e_2 + e_1)$$

$$\sigma_{12} = C_{44}e_{12}$$

$$\sigma_{13} = C_{44}e_{13}$$

$$\sigma_{23} = C_{44}e_{23}$$

The first conclusion is that for the isotropic material, the principal axes of stress (no shear) coincide with those of principal strain. Let $(C_{11} - C_{12})/2 = G$, and also $C_{12} = \lambda$. These are Lamé's elastic constants, G and λ . In stress tensor transformation from the principal axes to any arbitrary axes, C_{44} can be shown to be G . Or in tensor notation

$$\epsilon_{ij} = \frac{1}{E} [\sigma_{ij}(1+\nu) - \nu(\sigma_{kk})] \quad i = j$$

$$= \frac{2(1+\nu)}{E} \sigma_{ij} \quad i \neq j$$

Using the relations,

$$G = \frac{E}{2(1+\nu)},$$

$$E = \frac{G(3+2G)}{\lambda+G},$$

$$\nu = \frac{\lambda}{2(\lambda+G)}$$

APPENDIX B
THE ELASTIC WORK (ENERGY)

If the deformation is adiabatic, the work input is a point function (15,16). Then, the work is equal to the elastic energy U_e (12).

$$dU_e = \sigma_x (de_x) + \sigma_y (de_y) + \sigma_z (de_z) + \sigma_{xy} (de_{xy}) + \sigma_{xz} (de_{xz}) + \sigma_{yz} (de_{yz})$$

This is the change of the elastic energy per unit volume. For a linear relation between the stress and the strain, the complementary energy, $e_x (d\sigma_x) + \dots$, is equivalent to the energy itself, $\sigma_x de_x + \dots$.

Hence,

$$\frac{\partial U_e}{\partial \sigma_x} = e_x ,$$

$$\frac{\partial U_e}{\partial \epsilon_x} = \sigma_x$$

Using the linear isotropic stress-strain relations developed in Appendix A and performing the integration of the energy expression, we obtain the result:

$$U_e = W = \frac{1}{2E} (\sigma_{xx}^2 + \sigma_{yy}^2 + \sigma_{zz}^2) - \frac{\nu}{E} (\sigma_x \sigma_y + \sigma_y \sigma_z + \sigma_z \sigma_x) + \frac{1+\nu}{E} (\sigma_{xy}^2 + \dots)$$

TUFTS UNIVERSITY MECHANICAL ENGINEERING REPORT

NUMBER T.U.M.E.R. 67-3

AN ANALYTICAL AND EXPERIMENTAL STUDY OF MAGNETOSTRICTIVE
DELAY LINES

by Phillip Yang, January 1967

ABSTRACT

In an earlier report, (T.U.M.E.R. No. 66-2), an input-output relationship, derived for torsional signals in a magnetostrictive delay line, indicated that the output voltage was dependent upon the coil lengths, speed of propagation, and other factors. That analysis is extended here. Experimental data are reported, and compared to the predictions.

NOMENCLATURE

l_1	Input Coil Length, inches
l_2	Output Coil Length, inches
C	Speed of Propagation of Stress Waves, inch/second C_c , C_t in compression and in torsion modes
N_1	Number of turns of Input Coil
N_2	Number of turns of Output Coil
I_2	Direct Current in the nickel wire, Amperes
i	Pulse Current in the coil, Amperes
R	Resistance, Ohms
t_w	Width of pulse current, seconds
d	Distance between the input coil and the output coil
θ	Twist, radians
$g = \phi_0/\sigma$	Output coefficient of magnetic flux over stress, Gauss/psi
σ	Stress, pounds per square inch, or psi
ϕ_0	Magnetic flux change, Gauss
f	Input coefficient of stress over the Input Coil Magnetic flux; subscripts <u>c</u> or <u>t</u> referring to the compression or the torsional mode.

INTRODUCTION

The nickel delay line has been used in systems such as analog and digital computers as an information storage device and also in problems of speech recognition as an encoding and decoding device (1, 2, 3). The relationship between the output voltage and the input current of the delay line was the subject of many investigators (3, 4, 5). Among them, R. C. Williams did an elegant work in obtaining "the voltage response by Fourier transform methods for an input current step-function". Differently from what he claimed, his treatment was valid only, according to the author's opinion, for the special case of smooth continuous current signal, not for a step. He took $\frac{l_2}{c}$ to be infinitesimal without considering its validity. Since his condition, i.e., the width of the current pulse was of the same order of magnitude as $\frac{l_2}{c}$, did not allow that assumption, then $\frac{l_2}{c}$ has to be considered finite. This point, whether $\frac{l_2}{c}$ is finite or infinitesimal, will be looked into more deeply in later sections.

This report will carry a strong tone on the physical point of view. The voltage output may be shown in general as a function of the lengths of the input and output coil, $\frac{l_1}{c}$ and $\frac{l_2}{c}$ at a given current step. Usually, the lengths of the input and output coil were made small and equal to each other for a better resolution in the information processing. That did not mean that the lengths could not be made different for understanding of the problem. In fact, a four inch input coil was used to demonstrate the dependence of the voltage output in a large scale.

ANALYSIS

INPUT CURRENT AND STRESS WAVE GENERATION

If a step current was applied to the input coil of the nickel delay line, a compressional stress wave would be generated according to the Joule effect. That is also called magnetostriction. If the coil length was greater than its diameter, an unbalanced stress occurred near the end of the input coil instantaneously when the current step was put on. Thus, the stress waves (the disturbance of motion) started at the two ends of the coil. Similarly, the torsional stress waves could also be observed, if the delay line was biased with a D.C. current, in addition to the current step in the coil. In this case, the compressional stress wave was also there, but with a different speed of propagation. The direction of the magnetic flux due to the D.C. current was tangential. The step current gave an axial flux. The resultant of these two gave a helical strain, which was shown (6) to be equivalent to a twist (rotational displacement). This is often referred to as the Wiedemann effect. The rotational stress also started at the two ends of the long coil.

Actually, the coil length was smaller than its diameter in most applications. Hence the signal form was distributed and rounded off. However, in the following discussion, ideal conditions will be assumed for convenience. These conditions are (a) the coil length greater than the diameter; (b) the unbalanced force or torque was concentrated at the two ends of the coil; (c) the attenuation and dispersion effects were neglected; (d) the winding of the coil was uniform; and (e) the leakage of the magnetic flux was negligible.

Since the similarity existed between the compressional and the torsional stress waves, the following arguments would apply to both modes.

STRESS WAVE PROPAGATION AND OUTPUT VOLTAGE

Given a step function of current i , the two unbalanced forces at the two ends of the input coil, i.e., one at each end, would be a step function too. Considering either force first, it could act at any point along the delay line. Let that point be $x = 0$, at $t = 0$. At $t = t_0$, the wave fronts would be at $+x_0$ and $-x_0$, leaving behind the wave fronts a positive-stressed region and a negative-stressed region, as shown in Figure 1.a (7). The two unbalanced forces, which were separated by a distance of l_1 , and opposite in sign, would give the stressed regions as shown in Figure 1.b. There were a total of four wave fronts. Two were travelling in each direction and separated by a distance of l_1 .

The above discussions concerned a step current at the input coil. A pulse current of width t_w may be equivalent to the sum of two equal and opposite steps with a delay in time of t_w . Similarly, the stressed regions for a pulse current could be shown as in Figure 2. Furthermore, any continuous current input could be considered as a sum of a series of current pulses of any incremental width each with a delay in time.

An output coil downstream would give a voltage due to the motion of the stressed regions. The stress would result in the level change of the magnetic fluxes in the stressed regions (8, 9). As the stressed regions propagate along the nickel line, it could be viewed that the steady magnetic fluxes moved with the same speed of propagation. When the fluxes passed through the output coil, a voltage would be generated in proportion to the change of the fluxes with time experienced by the coil. Mathematically, the voltage at the pick-up

coil would be $V_2 = \frac{d\phi}{dt}$. But in carrying out the derivative, extra care should be exercised about the significance of the output coil length, l_2 , and the speed of propagation.

VOLTAGE OUTPUT OF FINITE LENGTH l_2

The length l_2 can be modeled to be either finite or infinitesimal. If the input current is of the pulse form, l_2 has to be considered to be finite. On the other hand, if the current is smooth and continuous, then we could consider l_2 to be infinitesimal as in the next section. Now, for the finite length l_2 of the output coil, we shall take the derivative of the magnetic fluxes with respect to time. The fluxes were proportional to the stress level of the stressed regions and the cross-sectional area of the nickel wire. When the stressed regions reach the leading edge of the coil, the coil could experience a change of fluxes with time. This change would be proportional to the speed of the stress wave propagation. Similarly, the coil will also experience a negative change of fluxes when any stressed regions leave the trailing edge of the coil or the exit. But when the stressed regions are moving inside the coil, they would give no change of fluxes with respect to time. With all these facts in mind, we could calculate the voltage V_2 for the case of $\frac{l_1}{c} = \frac{l_2}{c}$ which is greater than t_w shown in Figure 2.a. Let n_2 be the number of turns per unit length of the coil:

$$\begin{aligned}
 V_2 &= \frac{d\phi}{dt} = \lim_{\Delta t \rightarrow 0} \frac{n_2 (\Delta x) \phi_0}{\Delta t} \\
 &= n_2 \phi_0 c && \frac{d}{c} + t_w > t \geq \frac{d}{c} \\
 &= 0 && \frac{d}{c} + \frac{l_1}{c} > t \geq t_w + \frac{d}{c} \\
 &= -2n \phi_0 c && \frac{d}{c} + \frac{l_1}{c} + t_w > t \geq \frac{d}{c} + \frac{l_1}{c} \\
 &= 0 && \frac{d}{c} + \frac{2l_1}{c} > t \geq \frac{d}{c} + \frac{l_1}{c} + t_w
 \end{aligned}$$

$$V_2 = n_2 \dot{\psi}_0 c$$

$$\frac{d}{c} + \frac{2l_1}{c} + t_w > t \geq \frac{d}{c} + \frac{2l_1}{c}$$

The results were drawn in Figure 3.a and Figure 3.b for the cases of Figure 2.a and Figure 2.b. Similar results of Figure 4 could be compared with the experiments. These reasonings are quite different from other investigators', such as R. C. Williams', but surprisingly the results are the same.

One thing was significant: that the modulation by the input was quite the same as that of the output coil. Next, let's look into the case of infinitesimal length of l_2 .

VOLTAGE OUTPUT OF INFINITESIMAL LENGTH l_2

Since n_2 is infinite now, it cannot be used here. Let N_2 be the total number of turns of the SMALL output coil.

$$V_2 = N_2 \frac{d\phi}{dt}$$

where $\phi_0 = g_c \sigma$ in the compressional stress wave.

$$\sigma = f_c \frac{N_1 i}{l_1}$$

$$\text{Hence } V_2 = g_c f_c \frac{N_1 N_2}{l_1} \left[\frac{di}{dt} \Big|_t - \frac{di}{dt} \Big|_{t + \Delta t} \right]$$

This delay of Δt in the stress wave, σ , was from the input coil: i.e., $\Delta t = \frac{l_1}{c}$

Expanding the $\frac{di}{dt}$ in terms of the Taylor-series and neglecting the higher order

terms,

$$V_2 = g_c f_c \frac{N_1 N_2}{l_1} \frac{d^2 i}{dt^2} \frac{l_1}{c}$$

Similarly for the torsional stress wave, (6)

$$V_2 = g_t f_t \frac{N_1 N_2 I_2}{R C_t} \frac{d^2 i}{dt^2}$$

EXPERIMENTS

Whether the evidence provided by the test results support or reject the analysis depends very much upon knowledge of the testing conditions as well as the testing variables, such as the input current and the lengths of the coils. The current pulse to the four-inch coil shown in Figure 5 was fed from a pulse generator which gave a 12 volt pulse of 40×10^{-6} sec width at no load. The output voltage was stepped up by a transformer shown in Figure 6. Two kinds of reading at the secondary winding were taken and recorded, one at $R = 10^3$ and one at $R = \infty$. In other words, at $R = 10^3$ the current of the secondary winding was recorded; while at $R = \infty$ the open voltage taken was actually equal to the driving voltage of the primary winding if the voltage drop in the short circuit due to the resistance was neglected. The current form of the secondary winding was used in the delay line application and will be shown in the trace of Figure 7 and Figure 8 for comparison. Here, we are interested in the readings of $R = \infty$.

The length of the output coil, l_2 , was 1/8". Three input coil lengths, 1/8", 3/4", and 4" were used. In Figure 7 the upper trace was for the 1/8" input coil at $R = \infty$. The other three traces were at $R = 10^3$ for the 1/8", 3/4", and 4" input coils respectively. The same traces for 3/4" and 4" coils at $R = 10^3$ were in Figure 8 again. The bottom trace in Figure 8 was for the 4" coil at $R = \infty$. Figure 9 was of the 3/4" coil at $R = 10^3$ and $R = \infty$. The time scale for all the traces was 20×10^{-6} sec/cm. In all the traces, both the compressional stress waves and the torsional one were there. The compressional signal came first with its higher speed of $C_c = 2 \times 10^5$ in/sec and was shown nearer the zero time at the far left end of the trace. The torsional one followed with a speed of $C_t = 1.1 \times 10^5$ in/sec.

Looking at these traces, we could see that the voltage forms were depending upon the coil lengths and the speed of propagations, as we expected from Figure 4. For the input length of 4", $\frac{l_1}{c_c} = 20 \times 10^{-6}$ sec and $\frac{l_1}{c_t} = 36 \times 10^{-6}$ sec which were the times for each mode to delay and invert the current pulse. The current pulses consisted of two major peaks and one negligible small one with a total width of 8×10^{-6} sec. In Figure 8, the bottom trace of the four-inch coil confirms the expected modulation due to the input coil. The output coil length, l_2 , was 1/8" and $\frac{l_2}{c_c} = \frac{5}{8} \times 10^{-6}$ sec; $\frac{l_2}{c_t} = \frac{9}{8} \times 10^{-6}$ sec. It was not easy to count the output coil's modulation. Since the modulations of the output coil and input coil were the same, the effects of the output coil on the voltage signal could be observed from the numbers of peaks, the different delays of the compressional and the torsional modes and the change of the input coil lengths.

The current pulse had only two major peaks. The number of peaks in the compressional voltage was five, which was the result of delay shift of the output coil. The amount of delay shift in the torsional mode due to the same output coil was almost twice that of the compressional mode. Hence the torsional voltage form was also different. When the input length was short, 3/4" or 1/8", the modulations were messy. But the characteristics of the modulations were still there in Figure 9 and Figure 7.

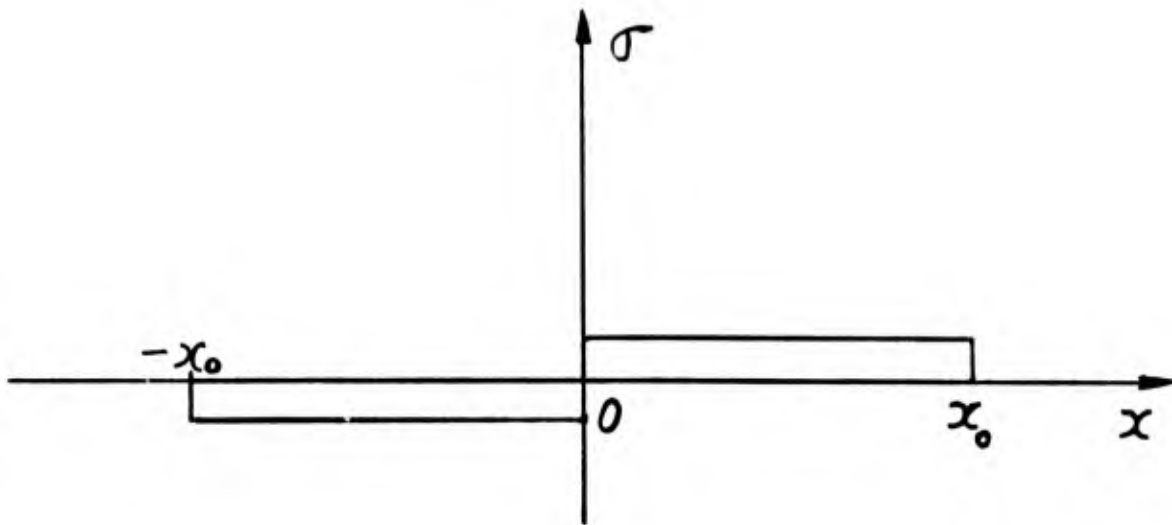
CONCLUSION

We have established that the output voltage of a delay line was dependent on the input coil length and the output coil length, the speeds of propagation, and the input current pulse. We have found that the modulation of the input coil was similar to that of the output coil. The propagation of the wave fronts and the motions of the stressed regions were made trivial here.

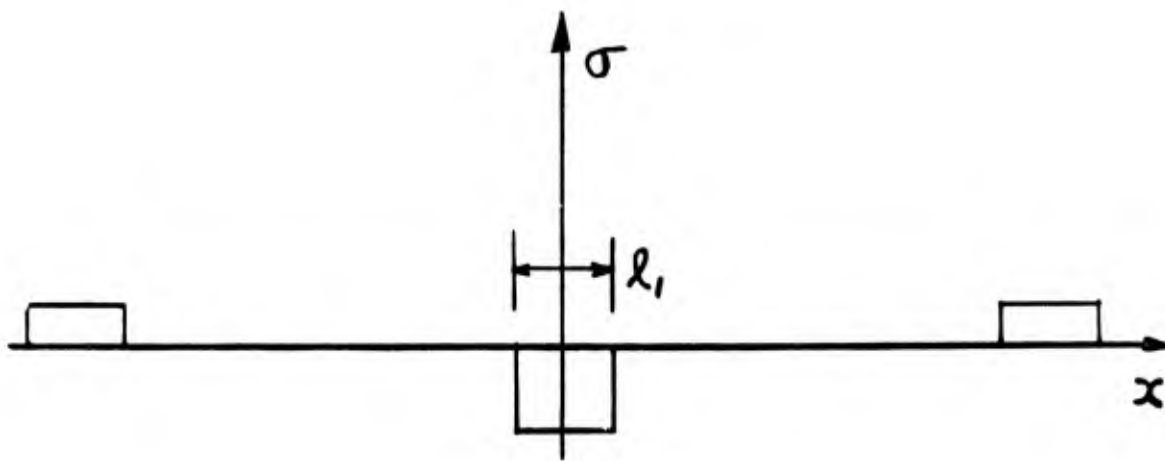
The significance between the models of the finite and infinitesimal lengths of the output coils was first pointed out here. Longer and different coil lengths were used for demonstration. The results confirmed to a great extent the expectations.

REFERENCE

- (1) Bradfield, G., "A New Electro-Acoustic Transducer"
Electronic Engineering Volume 20, pp. 74 - 78 March 1948
- (2) Robbins, R. C. and Millership, R. "Applications of Magnetostriction
Delay Lines" 1953 Proc. Symp. on Automatic Digital Computation.
National Physics Laboratory Teddington, England Pp. 199 - 212 1954
- (3) Epstein, H., and Stram, O. B. "A High-Performance Magnetostriction-
Sonic Delay Line" PGUE - 5 Transactions IRE p.5 August 1957
- (4) Williams, R. C. "Theory of Magnetostrictive Delay Lines for Pulse
and Continuous Wave Transmissions" IRE Transactions on Ultrasonics
Engineering PGUE - 7, pp. 16 - 38 February 1959
- (5) Tzannes, N. S. "Joule and Wiedemann Effects - The Simultaneous
Generation of Longitudinal and Torsional Stress Pulses in Magneto-
strictive Materials" IEE Transactions on Sonics and Ultrasonics
Vol. SU - 13 No. 2 July 1966
- (6) Yamamoto, M. "Theory of the Wiedemann Effect"
Science Report Tohoku University [A] 10, pp. 219 - 239 1958.
- (7) Shames, I. H. "Mechanics of Fluids" McGraw - Hill Company
Pp. 383 - 385 1962
- (8) Villan, E. "Change of Magnetization by Tension and by Electric Current"
Ann. Phys. Chem. Lp 2 126, Pp. 87-122 1965
- (9) Langenecker, B. "Inverse Magnetostriction Effect of Ultrasonic Stress
Waves in Steel" Journal of the Acoustical Society of America, Vol. 38
Pp. 234 - 238 August 1965
- (10) Philip Yang and Lloyd Trefethen " On the Electrical Generation and
Sensing of Rotational Stress Waves in Metal Wire Delay Line" T.U.M.E.R. 66-2
6 October 1966



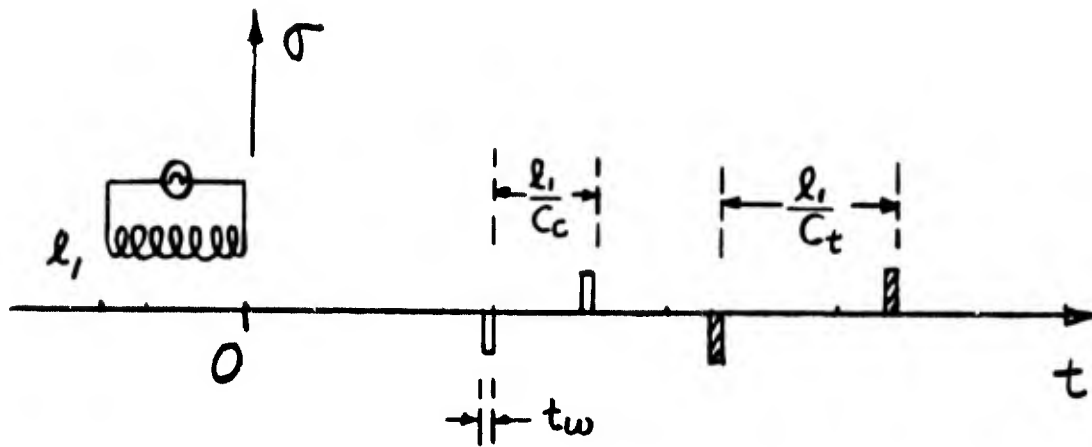
(a)



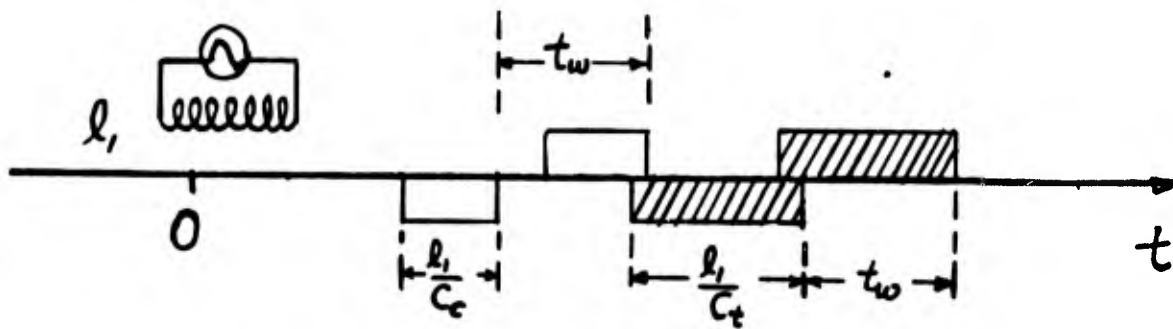
(b)

Figure 1 STRESSED REGIONS ALONG THE WIRE

- (a) Stress σ vs. Distance x at $t = t_0$
of a concentrated force at $x = 0$ $t = 0$
- (b) Actual stressed regions of a step current.



(a)



(b)

Figure 2 STRESSED REGIONS σ VS TIME t OF A PULSE CURRENT

$$(a) \quad \frac{l_1}{C_c} > t_w ; \quad \frac{l_1}{C_t} > t_w$$

$$(b) \quad \frac{l_1}{C_c} < t_w ; \quad \frac{l_1}{C_t} > t_w$$

Shaded Part For Torsional Wave

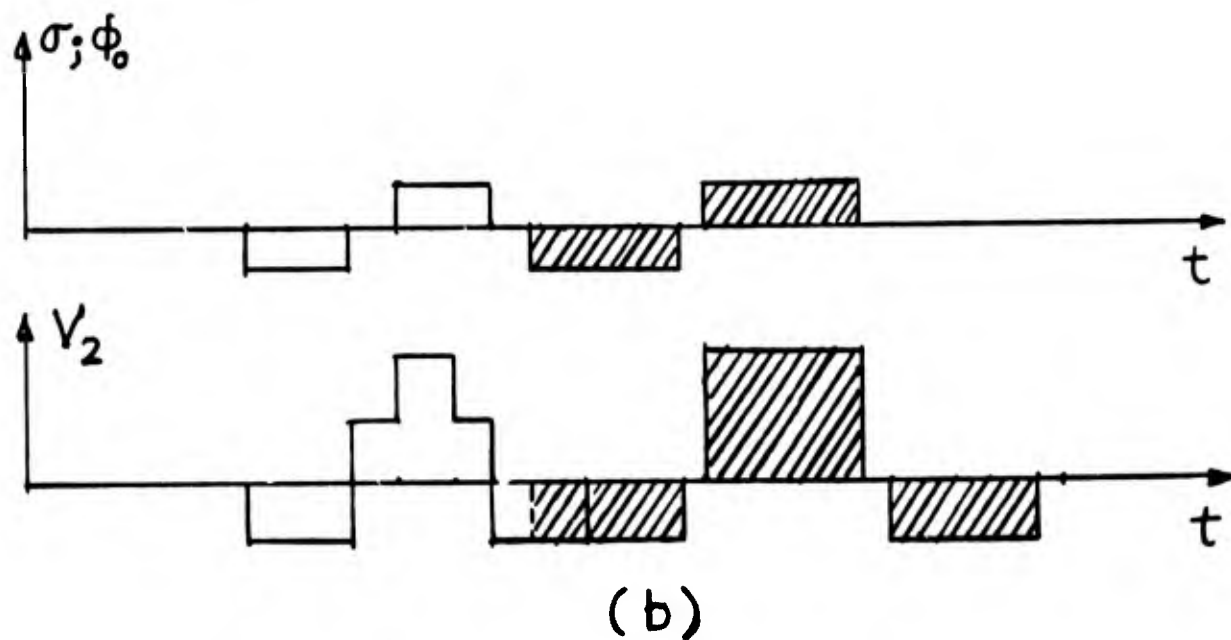
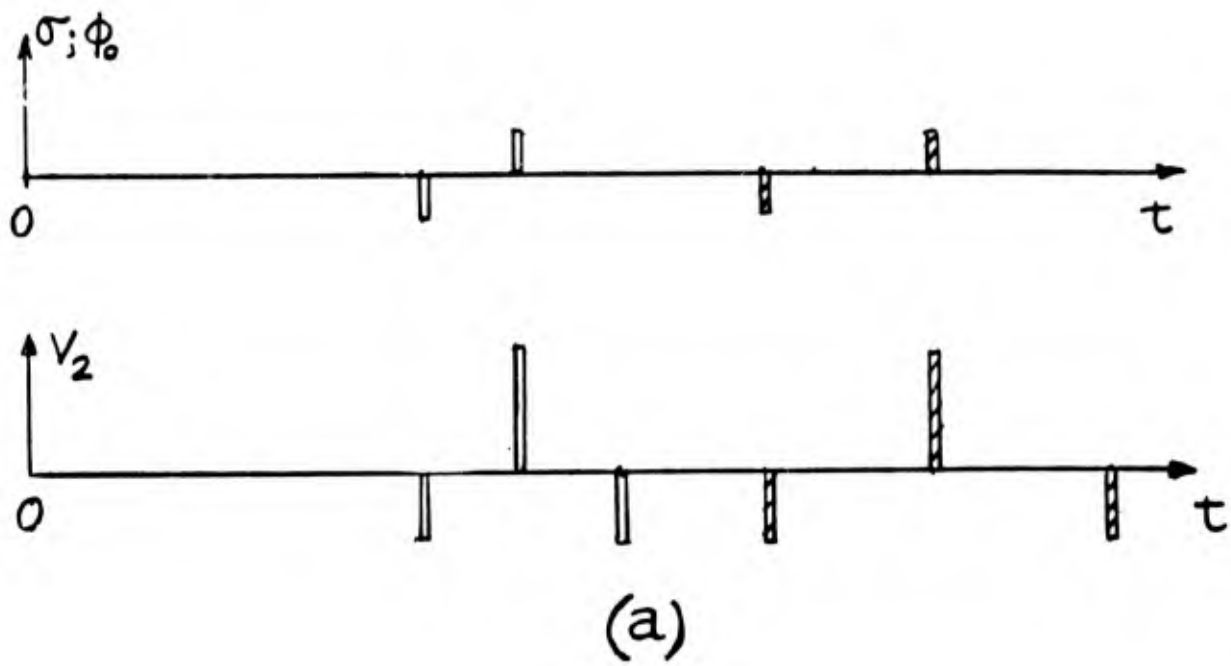


Figure 3 STRESS σ , MAGNETIC FLUX ϕ , AND OUTPUT VOLTAGE V_2

$$(a) \quad \frac{R_1}{C_c} = \frac{R_2}{C_c} > \tau_w ; \quad \frac{R_1}{C_t} = \frac{R_2}{C_t} > \tau_w$$

$$(b) \quad \frac{R_1}{C_c} = \frac{R_2}{C_c} < \tau_w ; \quad \frac{R_1}{C_t} = \frac{R_2}{C_t} > \tau_w$$

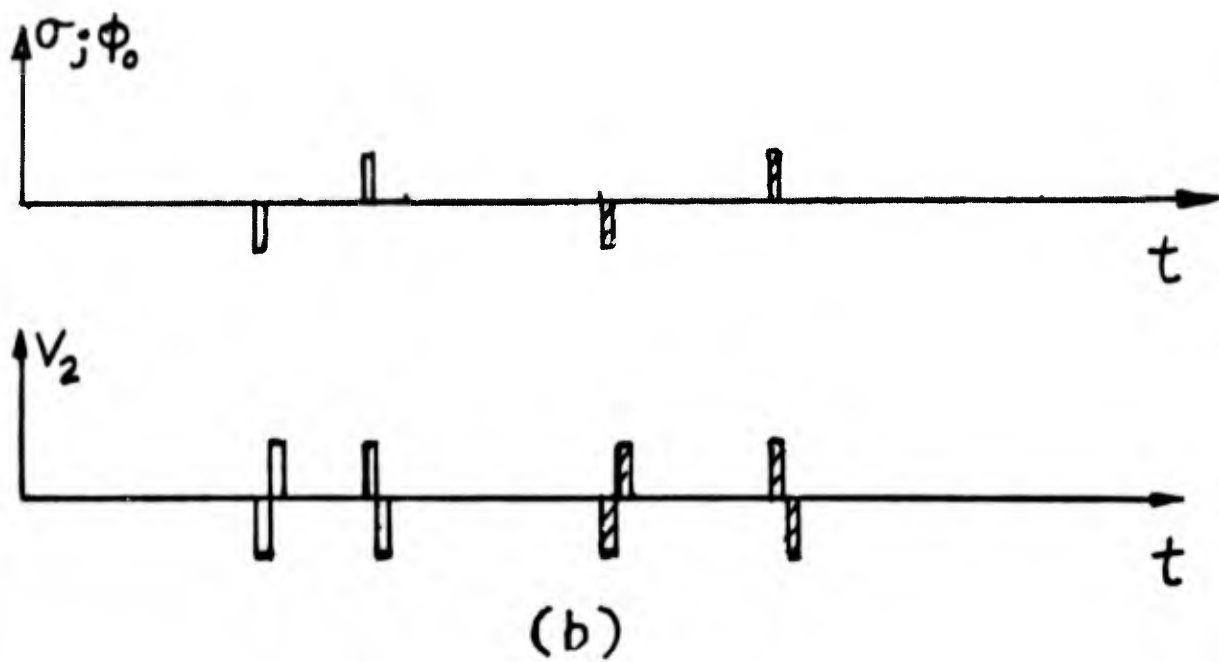
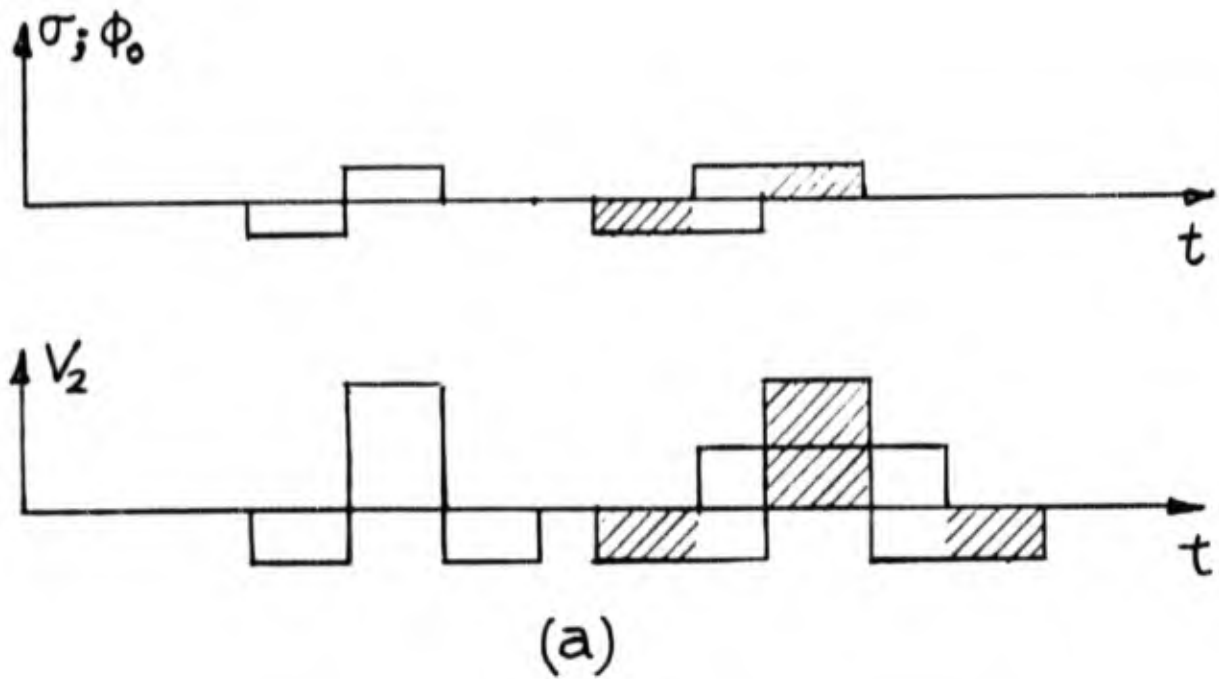


Figure 1. STRESS σ , MAGNETIC ϕ , AND OUTPUT VOLTAGE V_2

$$(a) \quad \frac{R_1}{C_c} = \frac{R_2}{C_c} = \tau_w ; \quad \frac{R_1}{C_t} = \frac{R_2}{C_t} > \tau_w$$

$$(b) \quad \frac{R_1}{C_c} > \frac{R_2}{C_c}, \quad \frac{R_2}{C_c} = \tau_w ; \quad \frac{R_1}{C_t} > \frac{R_2}{C_t} > \tau_w$$

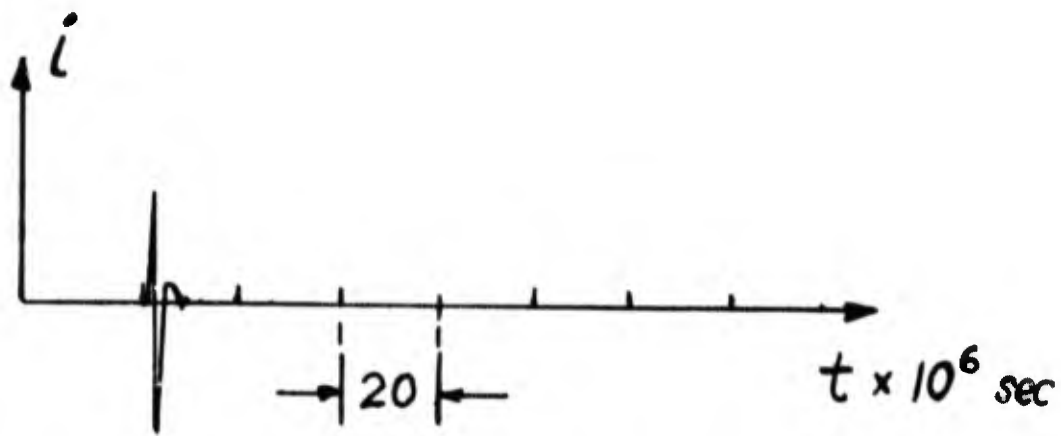


Figure 5 CURRENT PULSE i VS. TIME t

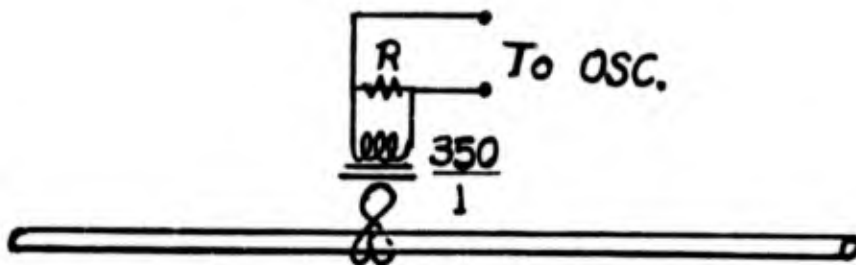


Figure 6 OUTPUT TRANSFORMER

$$R = 10^3 \text{ or } \infty$$

OSC - Oscilloscope

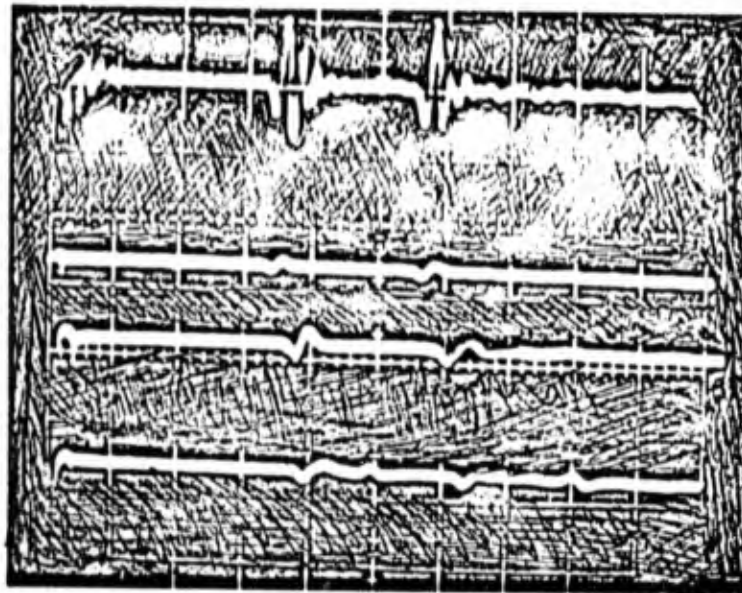


Figure 7 OUTPUT VOLTAGE vs. TIME

(a) 1/8" coil, $R = \infty$

(b) 1/8" coil, $R = 10^3 \Omega$

(c) 3/4" coil, $R = 10^3 \Omega$

(d) 4" coil, $R = 10^3 \Omega$

Time Scale, 20×10^{-6} sec/cm

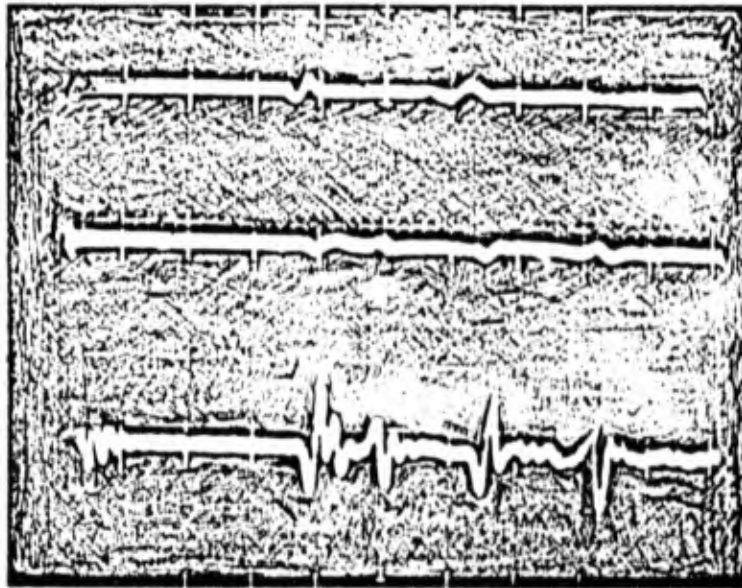


Figure 8 OUTPUT VOLTAGE vs. TIME

20×10^{-6} sec/cm

(a) $3/4$ " coll. $R = 10^3 \Omega$

(b) 4" coll, $R = 10^3 \Omega$

(c) 4" coll, $R = \infty$

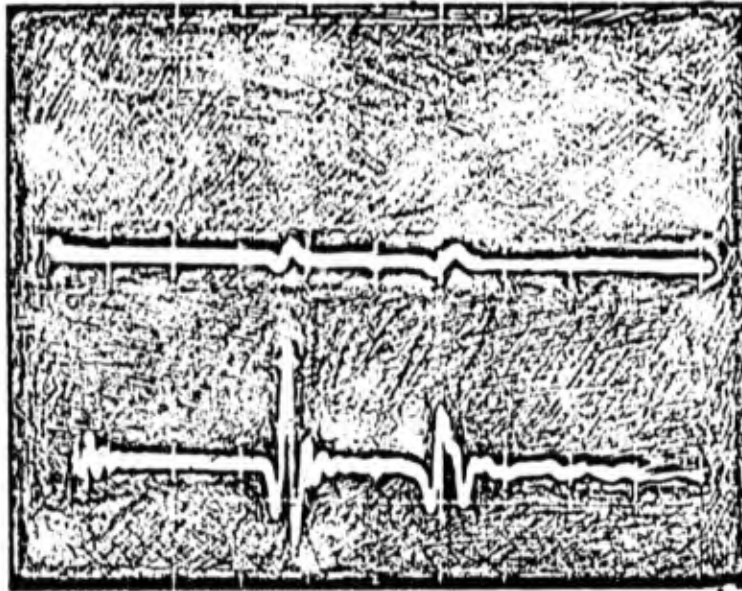


Figure 9 OUTPUT VOLTAGE vs. TIME OF 3/4" COIL

(a) $R = 10^3 \Omega$

(b) $R = \infty$

TUFTS UNIVERSITY MECHANICAL ENGINEERING REPORT

NUMBER T. U. M. E. R. 67-4

MAGNETIC CURRENT TWIST OF MAGNETOSTRICTION MATERIAL
CONTRASTED WITH WIEDMANN'S TWIST

by Philip Yang, February 1967

ABSTRACT

A current-carrying wire twists when subjected to the magnetic field of a surrounding solenoid. There are two causes of this twist, a magnetostrictive effect, the "Wiedemann" effect, and a torque interaction between the current and the solenoid fringing flux. This second effect has apparently not been previously considered. It is here shown that, for typical materials, this second effect is two or three orders of magnitude smaller than the Wiedemann effect. An experimental effort to detect this twist is reported; the results were useful in the sense that the twist was below the noise level, and therefore inaccessible, in the apparatus employed.

NOMENCLATURE

- \bar{J} Current density, Amperes/meter²
- \bar{n} Outward normal vector indicating direction only
- a;s Area, meter²
- V Volume, meter³
- \bar{B} Induced magnetic field density, Gauss/meter²
- \bar{H} Applied magnetic field density, Gauss/meter²
- μ Permeability constant
- $\bar{B} = \mu\bar{H}$
- N Number of turns of solenoid
- l Length of solenoid, meter
- I_1 Current to solenoid, Amperes
- I_2 Current through the nickel rod, Amperes
- R Radius of the nickel rod
- T Torque, Newton-meter
- θ Angular twist
- G Angular modulus of nickel, Newtons/meters²

INTRODUCTION

A nickel wire delay line was developed by D. W. Batteau (1), initially suggested from observations by Mechanical Engineering students in a senior projects laboratory course at Tufts University; subsequently, it was found that H. Whitehouse and others at N.O.T.S., Pasadena, had been working on such a delay line for some time. M. Whitehouse has suggested background references which gave some descriptions of the operational model of the delay line, i.e., the Wiedemann Effect of the magnetostrictive material. A different alternative model was attempted. A $\bar{J} \times \bar{B}$ twist existed, in addition to the presence of Wiedemann's twist. This alternative twist, which has been neglected without reasons, will be examined here. The relative magnitudes of each twist will be compared. Then, and only then, the less significant one will be dropped with justifications.

The observations originally made by students were that a nickel wire carrying a d.c. current was subjected to a rotational stress wave that travelled along the wire when a voltage pulse was applied to a short coil around the wire. The wave was observed in the voltage output from another coil placed some distance along the wire. Actually, two waves were observed, first a compression wave, followed by a slower torsional wave.

Batteau and Yang have made a number of experiments with these wires supported by a contract with N.O.T.S. It has been found that the torsional wave provides a convenient information carrier that allows for adjustable delay times, providing a device which could be of considerable use in information processing problems of interest in other research being conducted here.

Analysis of System

The system which was chosen to be analyzed was different in geometry and in character from the actual delay line. A static system contained the point of interest of the operational model of the delay line; i.e., the twist due to $\bar{J} \times \bar{B}$ we wished to examine. It was simpler than the dynamical characteristic delay line in which the unknown inertia and damping forces were involved. Simple geometry would undoubtedly make the calculations and the testing demonstrations easy. Any twist in a wire could be related to the external torque applied in a static system shown in Figure 1.

The input to the system was to have a current to the coil and a current to the wire (rod). The current on the coil may be related to the magnetic field surrounding the coil. The magnetic fluxes, \bar{B} , interacted with the current, \bar{J} , inside the nickel wire. As a result, $\bar{J} \times \bar{B}$ may be the force to produce the external torque about the wire axis. This will be continued in a later section. The magnetic flux inside the nickel wire, produced by the current coil, is governed by the static Maxwell Equation.

Static Magnetic Field and Maxwell Equation

The static Maxwell equations are

$$\oint \bar{H} \cdot d\ell = \iint_s \bar{J} \cdot \bar{n} da$$

$$\oint \bar{B} \cdot \bar{n} da = 0$$

$$\oint_c \bar{J} \cdot \bar{n} da = 0$$

$$\bar{B} = \mu H$$

The boundary equations

$$\bar{n} \times (\bar{B}_1 - \bar{B}_2) = \bar{K}_f$$

$$\bar{n} \cdot (\bar{B}_1 - \bar{B}_2) = 0$$

where K_f is the surface current density (Amperes per meter)

The magnetic fluxes satisfying both the Maxwell equations and the boundary condition are estimated as in the sketch of Figure 2, for the cylindrical wire or rod such as nickel, iron, or permalloys, surrounded by a long solenoid. The magnitude of the magnetic flux inside the nickel rod can be estimated from the following two simple cases of static magnetic problems. The first one is the magnetic flux produced by a long solenoid of air core and the second one is the "C-shaped" yoke of nickel or iron with a coil of many turns of winding wrapped around the yoke (Appendix A,B). Thus

$$B_a = \frac{K N I_1}{l}$$

$K = 1$ for the air core and $5 > K > 1$ for the nickel or iron core. For the condition $l \gg R$, the axial field density \bar{B}_a inside nickel will be uniform in the middle region of the coil. The radial components of the magnetic fluxes \bar{B}_r exist only near the two ends of the coil. Since the nickel rod is rotationally symmetric in geometry, so is the magnetic flux density \bar{B} .

The axial current density J in the nickel is a sum of the conducting current density J_{con} and a magnetic current density J_{mag} . (2). The magnetic current may be calculated as follows.

When the conducting current I_2 ($\pi R^2 J_{con}$) is supplied into the nickel rod of diameter $2R$, a large tangential magnetic field is set up in the nickel. On the other hand, with the same current supplied to a copper rod of the same diameter, a rather small magnetic field exists in the copper. The difference is the magnetic permeability constant. The large magnetic field in the ferromagnetic material, such as nickel, iron, cobalt and their alloys, can be explained by introducing the magnetization \bar{M} .

$$\bar{M} = \bar{B} - \bar{H}$$

$$\bar{J}_{con.} = \nabla \times \bar{H}$$

$$\bar{J}_{mag.} = \nabla \times \bar{M}$$

Since $\bar{J}_{con.} = \frac{I_2}{\pi R^2}$, $\bar{H} = \frac{J_{con.} \times \bar{r}}{2}$

Hence, $J_{mag.} = \frac{(\mu - 1) I_2}{2 \pi R^2}$

These results will be used in calculating the driving torque in the next section.

Torque and Angular Twist

The interaction of the total current density \bar{J} with the radial components of the magnetic fluxes \bar{B} will result in the torque expression first.

$$T_1 = \iiint (\bar{J} \times \bar{B}) \times \bar{r} dV$$

The value \bar{J} will be a sum of the conducting current density \bar{J}_{con} and a magnetic current density \bar{J}_{mag} , described in the early section. The direction of \bar{J} is parallel to that of the conducting one. It is uniform across the whole cross-sectional area in the nickel rod except at the cylindrical surface where singularity occurs. The magnitude of the opposite magnetic surface current would be equal to the product of the magnetic current density and the cross-sectional area. The net magnetic current in the nickel should be equal to zero besides the conducting one.

Having grasped the physical understanding of the quantities inside the above volume integral, we could carry out the integration easily.

$$\begin{aligned} T_1 &= \int_0^x \int_0^R \frac{\mu+1}{2} \frac{I_2}{\pi R^2} B_r(r,x,t) 2\pi r \cdot r \cdot dr dx \\ &= (\mu+1) \frac{1}{2} \frac{I_2}{R^2} \int_0^x \int_0^R B_r(r,x,t) r^2 dr dx \end{aligned}$$

The axial distance x is where the radial flux exists.

Now we assume the function of B_r to be separable, i.e.:

$$B_r(r,x,t) = f(r) g(x) h(t)$$

$$\int_0^x B_r(R,x,t) \cdot dx \cdot 2\pi R = B_a \cdot \pi R^2$$

where B_a is the uniform axial magnetic flux in the central portion of the solenoid and B_r is zero there.

$$\text{Similarly } \int_0^x B_r(r, x, t) dx = \frac{B_a r}{2} \\ = \frac{K N_1 i_1 r}{\ell_1^2}$$

$$\text{Thus, } T = \frac{(\mu+1)i_2}{R^2} \int_0^R \frac{K N_1 i_1 r}{\ell_1^2} r^2 dr$$

One can be dropped when $\mu \gg 1$.

$$\text{Finally, } T = T_1 = \frac{\mu i_2 K N_1 i_1 R^2}{8\ell_1^2}$$

The torque, T_1 , does not include the part contributed by the surface current interacting with the radial magnetic fluxes. That surface torque, T_s , is opposite to and twice in value to the T_1 .

$$T_s = - \int_0^x I_M B_r R dx$$

$$\text{where } I_M = J_M \cdot \pi R^2 = \frac{(\mu-1)}{2} i_2$$

$$\text{Hence, } T_s = - \frac{\mu i_2 K N_1 i_1 R^2}{4\ell_1^2}$$

Taking the algebraic sum of these two torques,

$$T_{\text{total}} = \frac{\mu i_2 K N_1 i_1 R^2}{8\ell_1^2}$$

The angular twist θ ,

$$\theta = \frac{T_{\text{total}} \ell_1}{G \Pi}$$

where $\Pi = (\pi R^4)/2$, the second moments of area, meter⁴.

After substitution,

$$\frac{\theta}{\ell} = \frac{\mu i_2 K N_1 i_1}{4\pi R^2 G \ell_1}$$

This twist will be compared with Yamamoto's next (3).

Comparison of Results

Yamamoto's twist:

$$\left(\frac{\theta}{\lambda}\right)_y = \frac{3}{R} \frac{\lambda N i_1 i_2}{\ell_1 2\pi R \left[\left(\frac{N i_1}{\lambda_1}\right)^2 + \left(\frac{i_2}{2\pi R}\right)^2 \right]}$$

where λ is the magnetostrictive coefficient

$$\lambda = 15 \times 10^{-6} \text{ at } H = 4 \text{ Gauss} = \frac{10}{\pi} \text{ Amp/cm for nickel.}$$

Comparing the order of magnitude of these two twists:

$$\frac{\left(\frac{\theta}{\lambda}\right)_{JxB}}{\left(\frac{\theta}{\lambda}\right)_y} \text{ Ratio} = \frac{12.6 \text{ K } \mu}{100 \text{ G } \lambda} \left[\left(\frac{N i_1}{\lambda_1}\right)^2 + \left(\frac{i_2}{2\pi R}\right)^2 \right]$$

where $\frac{12.6}{100}$ is the conversion factor (Appendix C)

$$\text{Hence, Ratio} = \frac{2}{1500} ,$$

$$\text{when } K = 5, \mu = 500, G = 10^{11} \left[\frac{\text{Newton}}{\text{m}^2} \right] = 10^{12} \left[\frac{\text{dynes}}{\text{cm}^2} \right]$$

$$\lambda = 45 \times 10^{-6} \frac{N i_1}{\lambda_1} = 20 \text{ Amp/cm} \quad \frac{i_2}{2\pi R} = 1 \text{ Amp/cm}$$

Hence, the J x B twist, $\left(\frac{\theta}{\lambda}\right)_{JxB}$, is shown not significant in the nickel delay line.

Discussion

The testing condition of the Wiedemann twist was such that the presence of the magnetic current twist was always unexclusive. It gave a suspicious possibility that the Wiedemann twist might be magnetic rather than magnetostrictive.

When a nickel wire was long enough so that the two ends of the nickel wire were outside the solenoid, the magnetic twist due to the introduction of the radial flux component of the solenoid and the magnetic current of the nickel wire was there as well as the magnetostriction twist. On the other hand, when the nickel wire was shorter than the length of the solenoid and was placed completely inside the solenoid, the axial flux component of the solenoid could interact with the radial surface current (magnetic) of the nickel wire. As a result, a twist of equal magnitude as the first case was also there. For the passage of the conducting current in the second case, the ends of the nickel wire were connected to two copper wires extending away from the ends of the solenoid (4). Now, the calculation made in this study excluded that suspicious possibility.

FEASIBILITY OF EXPERIMENTAL DEMONSTRATION

In order to have greater confidence in the analysis, it is worthwhile to look into the demonstrations of the analytical results and its feasibility. Any ferromagnetic material of high permeabilities and low magnetostriction constants would satisfy the requirement - i.e., the large contrast between these two twists considered in the section of Comparison of Results. Carpenter Steel Company supplied us with their HiMu-80 alloy, its permeability being approximately 10,000 before saturation. Its magnetostriction constant was unknown, but could be measured. These two twists could also be separated. The diameter of the stock we received was 7/16". Any other smaller size was possible but not available.

The sensing element of the magnetic twist to be measured consisted of a telescope, a mirror, and a scale. The distance L between the mirror attached to the free end of the nickel rod above the mercury pool and the scale was about 40 feet. With a surveying telescope, a 0.05 in. (on the scale) resolution could be observed.

The angle of twist would be

$$\theta = \frac{12.6}{100} \frac{N_1 i_1}{l_1} l_1 \frac{i_2 K \mu}{4\pi R^2 G} \quad \text{radians}$$

Letting $\frac{N_1 l_1}{l} = 40 \text{ Amp/cm.}$

$$i_2 = 40 \text{ Amp.}$$

$$R = 0.3 \text{ cm.}$$

$$G = 10^{12} \text{ dynes/cm}^2$$

$$l_1 = 210 \text{ cm.}$$

$$\mu = 10,000$$

$$K = 5$$

$$\theta = 40 \times 10^{-5} \text{ radians}$$

The linear displacement, x , detected in the 40 ft. away scale, would be

$$x = 2\theta L = 4 \times 10^{-1} \text{ in.}$$

The above optimistic number was not realistic, since the saturation of the magnetic fluxes due to the $i_2 = 40$ Amp. occurred much sooner. The non-linear region of the magnetic fluxes started at $H = 0.01$ gauss or $H = 0.01 \times \frac{10}{4\pi}$ Amp./cm.

$$2\pi RH = i_2$$

Hence $i_2 = 2.4 \times 10^{-2}$ Amperes was the upper bound for $R = 0.3$ cm. in the linear region.

When $i_2 = 5 \times 10^{-2}$ Amperes was used, the angle of twist would be too small to be detected.

The stiffness of the nickel rod was too large when $R = 0.3$ cm. The smaller the diameter the larger the twist would be. When $R = 2.5 \times 10^{-3}$ in., or $R = 6 \times 10^{-3}$ cm., $x = 4 \times 10^{-2}$ inches, which was still below the noise level of the system. If the 7/16" nickel rod was cut into two halves and these two nickel rods were connected to a thin copper wire, the copper wire in the middle was for less stiffness and the nickel rod for torques. Unfortunately, the magnetic current torques cancelled themselves, and the net torque would be zero in this case of feasible stiffness except the negligibly small one which resulted from the conducting current.

If we increase the sensitivity of the sensing element, e.g., let $L = 80$ feet, the signal to noise ratio would still be too small. In other words, the random vibration of the room gave a noise level of approximately $\theta = 10^{-4} \sim 10^{-3}$ radians.

In summary, the analytic result could not be easily demonstrated under the limitations of stiffness, the saturation, the nature of the magnetic current, and the noise level.

REFERENCE

- (1) Batteau, D.W. and Flanagan, G.P. "A Study of Acoustical Multipath Systems, Section IV, Delay Line" 1 June 1966 Final Report: Contract NONR 494(00) U.S. Navy Office of Naval Research
- (2) Feynman, Leighton, and Sands, "The Feynman Lectures on Physics" Vol. 2.
- (3) Yamamoto, M. "Theory of the Wiedemann Effect" Science Report Tohoku University [A] 10, pp.219-239, 1958
- (4) Williams, S.R. "A Study of the Joule and Wiedemann Magnetostrictive Effects in Steel Tubes" Physics Review 32, pp. 281-296, 1911

APPENDIX A

Magnetic Field in Air Produced by a Long Solenoid

A solenoid of length L , radius R , and n turns per unit length may be considered to be long when $L \gg R$, such as $L = 100 R$. If we assume that the current-carrying wire is closely spaced, the magnetic field may be in general calculated from the Biot-Savart Law, i.e.:

$$d\bar{B} = \frac{I d\vec{l} \times \bar{S}}{4\pi S^3}$$

where $d\bar{B}$ is the incremental flux due to the current-carrying segment $d\vec{l}$.

I is the current whose direction is parallel to the segment $d\vec{l}$.

\bar{S} is the distance from the segment $d\vec{l}$ to the point at which the field flux $d\bar{B}$ is calculating.

Thus, the contribution to \bar{B} from any short segment of wire $d\vec{l}$ can be taken to be a vector perpendicular to the plane containing $d\vec{l}$ and \bar{S} .

Since the flux \bar{B} along the axis of the long solenoid is easy to calculate and the result of it will help to estimate the pattern of variation of fluxes at different locations, we are going to calculate the field along the axis. This consists of two steps. Breaking the length of the solenoid into small segments of rings and considering the flux due to a ring-segment, we may obtain first the following equation describing the field flux on the axis at any point z above or below the ring-segment, by the Biot-Savart Law.

$$B_z = \frac{2\pi R^2 I}{S^3} = \frac{2\pi R^2 I}{(R^2 + z^2)^{3/2}}$$

Next, the contribution from the ring-segment included between radii from the point z making angles θ and $\theta + d\theta$ with the axis, is

$$dB_z = \frac{2\pi R^2 I \sin\theta d\theta}{S^3}$$

Since the length of the ring-segment of the solenoid is $S d\theta / \sin\theta$ and is equivalent to a ring carrying a current of $I n S d\theta / \sin\theta$. Integrating over the limits of θ_1 and θ_2 , the angles between the radii (extending from the point z to the two ends of the coil) and the axis,

$$E_z = \int_{\theta_1}^{\theta_2} \frac{2\pi I n R^2 d\theta}{S^2 \sin\theta} = 2\pi I n \int_{\theta_1}^{\theta_2} \sin\theta d\theta$$

since $\sin\theta = \frac{R}{S}$

$$B_z = \frac{\mu_0 I n}{2} (\cos\theta_1 - \cos\theta_2)$$

For an infinitely long solenoid, $\theta_1 = 0$, and $\theta_2 = \pi$

$$B_z = \mu_0 I n = \frac{\mu_0 N I}{L}$$

One of the properties of the infinitely long solenoid is that the flux density is uniform everywhere inside the solenoid. It is independent of z , the coordinate in the axial direction, and is equal to $\frac{\mu_0 N I}{L}$. The magnetic fluxes outside the solenoid may be shown to be zero.

Using the derived equation, the axial fluxes can be plotted as in Figure A-1 for a finite long solenoid, $L = 100 R$. The flux inside one-radius away from either end of the solenoid can be seen as 85% of that of the infinitely long solenoid; while the flux outside one-radius away is 15% of $\frac{\mu_0 N I}{L}$ along the axis.

APPENDIX B

Magnetic Fluxes in a "C-Shaped" Yoke of Nickel

Figure 3 is a "C-shaped" yoke of nickel wrapped by a coil around the yoke. If the gap thickness is small compared with the other dimensions, we can assume that the fluxes will go around through the loop just as they did in the torus. If the yoke has a uniform cross-sectional area and if we neglect any edge effects at the gap, we find B is uniform around the yoke. B will also have the same value in the air gap. Using the static Maxwell equations,

$$H_1 \ell_1 + H_2 \ell_2 = N I$$

calling H_1 the field in the air gap, ℓ_1 the gap thickness and similarly using 2 subscript for the nickel part. In the air gap, $d_1 = B_1$. Since $B_1 = B_2$, the above equation becomes

$$B_2 / \mu + H_2 \ell_2 = N I$$

Also $B_2 = \mu H_2$

The two unknowns, B_2 and H_2 , may be solved from the two equations. If the lengths ℓ_1 , ℓ_2 are equal, and μ is large, the part due to the nickel resistance, $H_2 \ell_2$, may be dropped. Hence the main resistance is contributed from the air gap, $H_1 \ell_1 = N I$.

The situation of a finite solenoid around a straight nickel rod is different from the "C-shape" yoke. The air path is larger than the nickel path. The flux density is not uniform either. But the resistance concept remains. For a magnetic material of large permeability, it offers less resistance to the magnetic flux than the air gap (path). If the small resistance can be neglected in the nickel rod, the length of the air path may be a fraction of that in the finite solenoid of air core. The perturbation of the fluxes by the presence of a nickel rod is assumed small. Then, it is the fraction of the resistance that contributes the factor K . The value of K may only be estimated as approximately $K = 2$.

APPENDIX C

Conversion Factor of $4\pi/100$

The basic relations between the force, the magnetic flux, and the current are

$$F = B I_2 L \quad [\text{Newton}] = \left[\frac{\text{Weber}}{\text{m}} \right] [\text{Amp}][\text{m}]$$

$$B \cdot L = \frac{4\pi}{10^7} N_1 I_1 \quad \left[\frac{\text{Weber}}{\text{m}} \cdot \text{m} \right] = \frac{4\pi}{10^7} [\text{Amp}]$$

Hence

$$F = \frac{4\pi}{10^7} N_1 I_1 I_2 \quad [\text{Newton}] = [\text{Amp}][\text{Amp}]$$

$$[\text{Newton}] = 10^5 [\text{dynes}]$$

$$F = \frac{4\pi}{10^7} 10^5 N_1 I_1 I_2 [\text{dynes}]$$

$$= \frac{12.6}{100} N_1 I_1 I_2$$

$$T = F \cdot L \quad [\text{Torque}] = [\text{dynes}][\text{cm}]$$

$$\theta = \frac{T \ell}{GK} \quad [\text{radian}] = \frac{[\text{dynes}][\text{cm}]^2}{[\text{dynes}][\text{cm}]^2}$$

$$\frac{12.6}{100} \frac{N_1 I_1 I_2 K(\mu+1)}{4\pi R^2 G} \quad [\text{radian}]$$

$$\text{When } G = \left[\frac{\text{dynes}}{\text{cm}^2} \right] \quad R = [\text{cm}] \quad I_1, I_2 = [\text{Amp}]$$

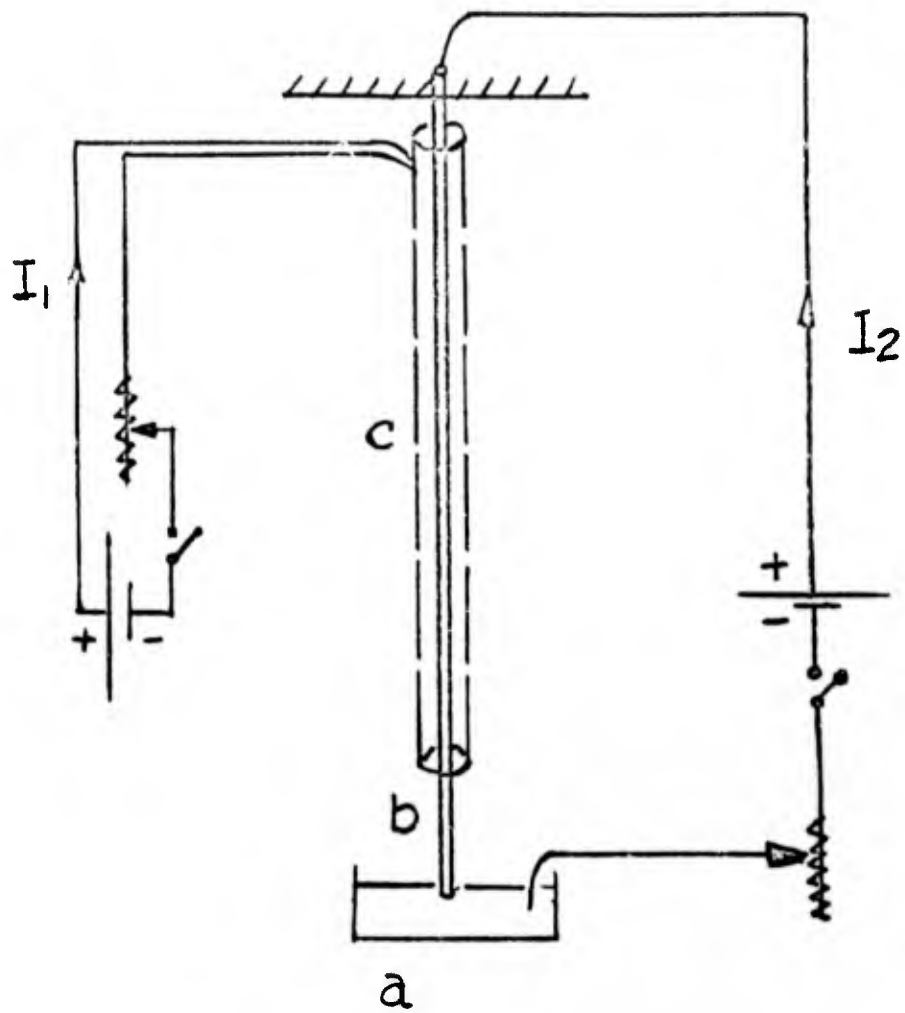


Figure 1 Static System Analyzed

- (a) Mercury Pool
- (b) Nickel Rod
- (c) Long Solenoid Coil

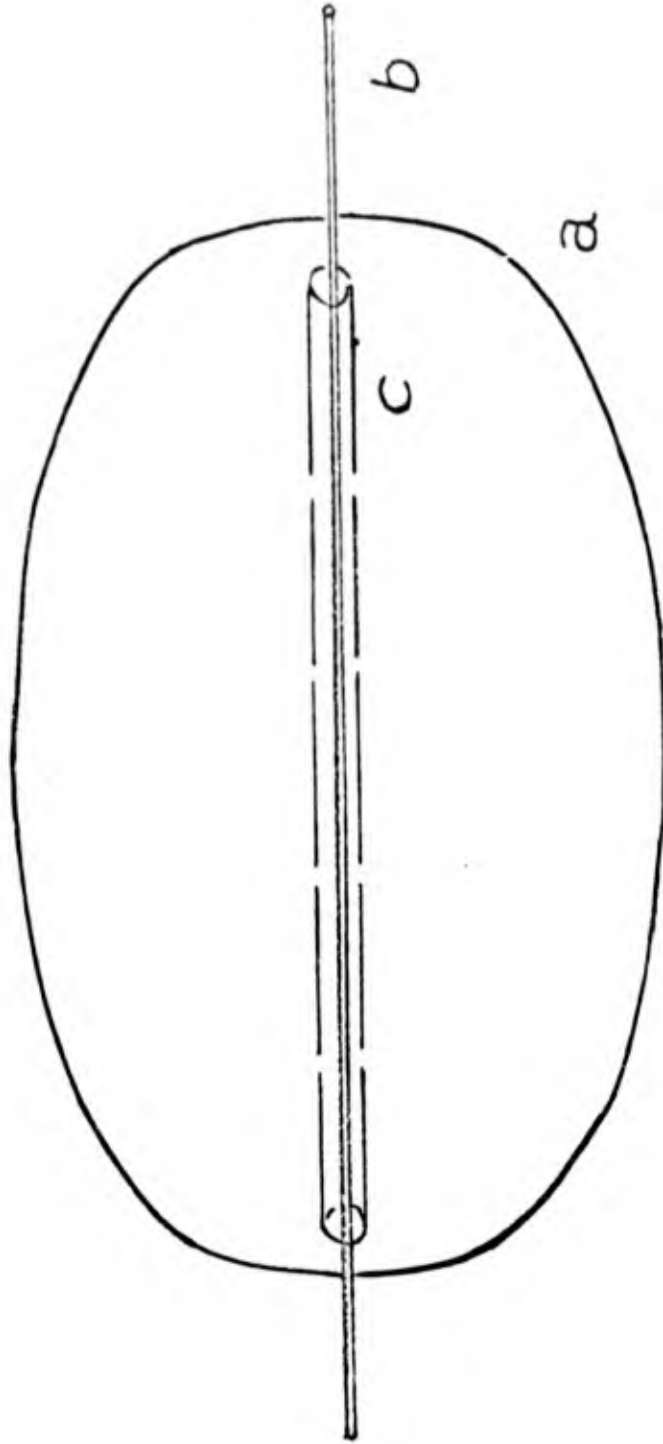


Figure 2 Estimated Magnetic Fluxes

- (a) Symmetric Fluxes
- (b) Nickel Rod
- (c) Long Solenoid Coil

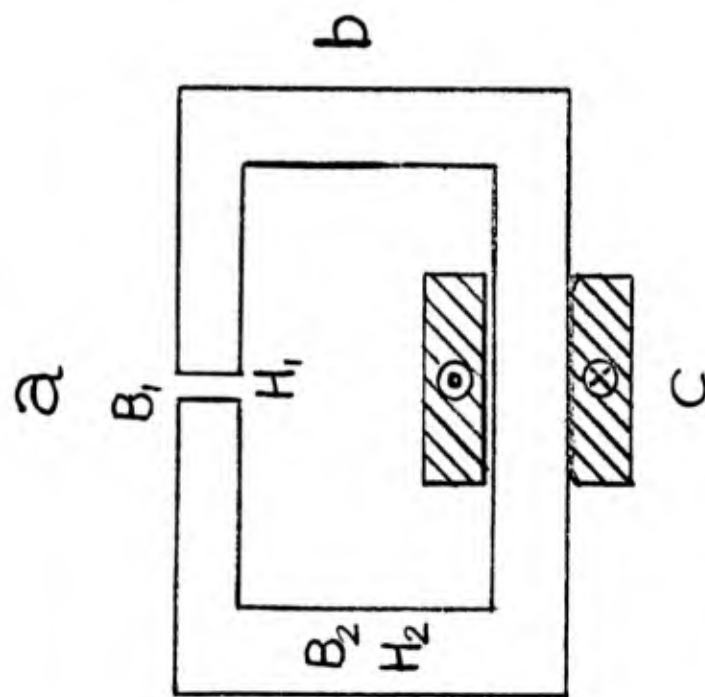


Figure 3 C-Shaped Yoke

- (a) Air gap
- (b) Nickel yoke
- (c) N-turns winding of current I

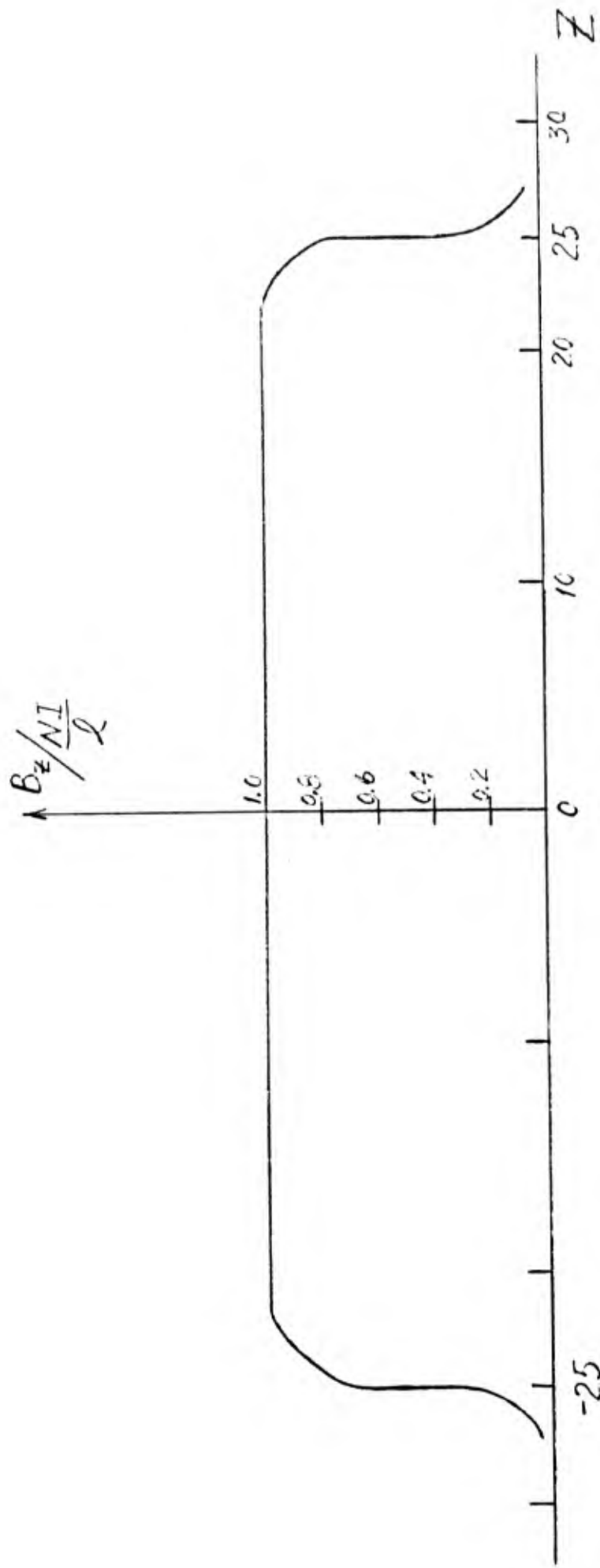


Figure A - 1 Axial Magnetic Fluxes vs. Distance Z
of a Long Solenoid, $L = 50 R$.

$Z = \pm 25 R$ The ends of the Solenoid